Mechanistic insights into effect of surfactants on oral bioavailability of amorphous solid dispersions

A. Schittny, S. Philipp-Bauer, P. Detampel, J. Huwyler, M. Puchkov

PII: S0168-3659(20)30050-X

DOI: https://doi.org/10.1016/j.jconrel.2020.01.031

Reference: COREL 10127

To appear in: *Journal of Controlled Release*

Received date: 14 August 2019

Revised date: 5 December 2019

Accepted date: 17 January 2020

Please cite this article as: A. Schittny, S. Philipp-Bauer, P. Detampel, et al., Mechanistic insights into effect of surfactants on oral bioavailability of amorphous solid dispersions, *Journal of Controlled Release* (2019), https://doi.org/10.1016/j.jconrel.2020.01.031

Mechanistic Insights into Effect of Surfactants on Oral Bioavailability of Amorphous Solid Dispersions

A. Schittny[1,2], S. Philipp-Bauer[1], P. Detampel[1], J. Huwyler[1], M. Puchkov[1]

[1]*Division of Pharmaceutical Technology, Department of Pharmaceutical Sciences, University of Basel, Switzerland*

[2]*Division of Clinical Pharmacology and Toxicology, Department of Biomedicine, University Hospital Basel and University of Basel, Switzerland*

1 Abstract

Drug delivery of poorly soluble drugs in form amorphous solid dispersions (ASDs) is an appealing method to increase in vivo bioavailability. For rational formulation design, a mechanistic understanding of the impact of surfactants on the performance of ASD-based formulations is therefore of importance.

In this study, we used hot-melt extrusion to prepare ASDs composed of the model drug substance efavirenz with hydroxypropyl methylcellulose phthalate (HPMCP) as the base polymer, and surfactants. Molecular dynamics simulations and in vitro dissolution studies were used to investigate formation and drug release from polymeric vesicles, and their ability to maintain a supersaturation state as a function of surfactant composition.

It was possible to identify main factors regulating particle formation and to modify dissolution profiles with different excipient compositions. Animal studies in the rat, in combination with physiologically based pharmacokinetic modeling, demonstrated enhanced drug absorption from formed vesicles. The surfactant composition in the ASD had a direct influence on the morphology of these vesicles, as well as kinetics of drug release, and, therefore, the oral bioavailability. ASDs, prepared by hot-melt extrusion method, were optimized for dissolution and adsorption rates increase.

Our findings contribute to a better understanding of dissolution behavior of ASDs with respect to the function of surfactants, aiming to facilitate a rational formulation development and an accelerated transition from in vitro systems to in vivo applications.

Keywords: Amorphous solid dispersion, poorly water-soluble drugs, bioavailability, formulation development

2 Introduction

Recurrent drop-outs of poorly soluble drug candidates during drug development [1] due to low bioavailability [2] create a need for delivery systems that improve drug solubility. A potential solution to decrease this attrition rate, i.e.,fraction fo drugs that are excluded during drug development, is a drug delivery in the form of amorphous solid dispersions (ASDs) [3]. ASDs are systems in which an active pharmaceutical ingredient (API) is stabilized by amorphous embedding into a solid polymer matrix [4]. Their use in oral drug delivery can increase *in vivo* bioavailability in animals and humans [5]. Although different methods exist to produce ASD [6], hot-melt extrusion has gained an increasing attention in formulation development. This process has an advantage of solvent-free and continuous processing [7]. During the extrusion process, polymer and API powder mixtures are fed to the extruder with subsequent melting and mixing to initiate dissolution and dispersion of the API crystals in the molten polymer. The molten mass is extruded through a die and is cooled down [8,9].

Enhanced bioavailability through ASDs is considered to result mainly from the temporary formation of a supersaturated solution of the active pharmaceutical ingredient (API) stabilized by polymer. It is, thus, possible to overcome the limitations of poor aqueous solubility. During the first dissolution phase of this process, supersaturation conditions are archieved by putting of an API in an amorphous state, i.e., a higher energy state as compared to crystalline conformation. The second dissolution phase is characterized by a stabilization of a supersaturation effect, ideally for a period of time sufficient to ensure complete absorption of the API in the gastro- intestinal tract (GIT) [10]. Different stabilization mechanisms such as solubilization as micelles with amphiphilic polymers, recrystallization inhibition by polymers [11,12], or the formation of colloidal drug-rich particles have been reported. Latter can be in a form of amorphous droplets, amorphous particles, or gel-like particles [13]. Such particles have higher drug loads [14,15] and are formed e.g. by liquid-liquid phase separation (LLPS) [16–18] or glass-liquid phase separation (GLPS) [19]. Here, based on mostly hydrophobic interactions, a meta-stable equilibrium between a supersaturated solution and a droplet phase containing the poorly soluble API and excipients is generated. Also, mixtures of different particle species have been observed [20,21]. The formation of drug-rich particles are still poorly understood. It should be noted that the choice of polymers directly influences if and what kind of drug-rich particles are formed. Studies on drug flux through membranes [12,22] revealed that polymer properties also influence flux trough the membrane[23]. Enhancements of drug flux have been reported [24–26] along with the absence of such effects [27]. Besides selecting different base polymers for binary formulations, an alternative formulation strategy is the compounding with excipients, such as other polymers or surfactants [28].

Different base polymers are reported as suitable carriers in ASDs [10]. While some have been developed specifically for use in ASDs, others have been used in pharmaceutical development for other purposes. An example of a known polymer that has not been designed for ASDs is the hydroxypropyl methylcellulose phthalate (HPMCP). It was initially developed for gastro-protective coating of tablets and has attracted little attention for application in ASD-based formulation design. It is available as HPMCP HP50 and HPMCP HP55, corresponding to its degree of phthalate substitution and therefore to the minimal pH-value (5.0 or 5.5) above which it becomes water-soluble [29,30]. These properties, i.e.,pH-dependent dissolution, makes it an interesting polymer for use in gastro-protective formulations of acid-sensitive APIs [31].

Surfactants can affect the performance of ASD formulations in different ways [4,10]. With respect to dissolution properties, surfactants were shown to enhance wetting [32], improve dispersibility [33], inhibit crystallization [34,35], stabilize the amorphous state of APIs [20], and enhance dissolution and supersaturation in general [36]. On the downside, the presence of surfactants in ASDs can also lead to inhibition of dissolution rates [33], can promote undesired crystallization as well as leaching of API from the drug-rich particles into the surrounding medium [35,37], and can influence particulate species formation [20,38].

APIs with a low bioavailability due to poor aqueous solubility can benefit best from a formulation as ASD. Efavirenz is such a drug that frequently has been used as a model compound in solubility enhancement studies [39–45]. Having a low solubility and high permeability, efavirenz is generally classified as a class II drug in the biopharmaceutical classification system (BCS) for doses of 600 mg in humans [46]. However, due to varying results in permeability measurements, a classification as BCS class IV drug is also possible [47].

Despite numerous research efforts to better characterize the dissolution process of ASDs, we still do not fully understand mechanisms of drug-rich particle formation, the effect of admixed surfactants, and factors influencing *in vivo* bioavailability. In this study, we therefore investigated the impact of admixed surfactants on the dissolution behavior and *in vivo* bioavailability of ASDs by experimental work and subsequent mechanistic analysis, aiming to contribute to the elucidation of API absorption from ASDs. We optimized and characterized drug-rich particle forming ASDs composed of HPMCP, surfactants, and efavirenz by microscopic particle imaging and molecular dynamics (MD) simulations, pharmaceutical dissolution testing and mechanistic data fitting, as well as *in vivo* bioavailability assessment in rats with physiologically based pharmacokinetic (PBPK) model fitting.

3 Materials and Methods

3.1 Chemicals

HPMCP HP50 and HP55 (hydroxypropyl methylcellulose phthalate) was kindly provided by Shin-Etsu Chemical Co., Ltd. (Tokyo, Japan). Efavirenz was obtained from Hetero Labs Limited (Hyderabad, India). Soluplus (polyvinyl caprolactam-polyvinyl acetate-polyethylene glycol graft copolymer) and Kollicoat IR (polyvinyl alcohol-polyethylene glycol graft copolymer) were kindly provided by BASF SE (Ludwigshafen, Germany). Kolliphor EL (polyoxyl 35 hydrogenated castor oil) and ethyldiglycol (Transcutol P), ammonium bicarbonate, ammonium hydroxide solution 28%, sodium hydroxide, EDTA (ethylenediaminetetraacetic acid) and methanol were ordered at Sigma-Aldrich Chemie GmbH & Co. KG (Karlsruhe, Germany). Ethanol 96%, Tween 80 (polysorbate), potassium dihydrogen phosphate, acetonitrile, and PEG 400 (poly-ethylene glycol) were purchased from Carl Roth GmbH & Co. KG (Karlsruhe, Germany). PEG 6'000 (poly-ethylene glycol) and formic acid were ordered from Merck KGaA (Darmstadt, Germany) and PEO 100'000 from (poly-ethylene oxide) from Alfa Aesar GmbH & Co. KG (Karlsruhe, Germany). Sucrose palmitate was obtained from Mitsubishi-Chemical Foods Corp. (Tokyo, Japan). Sterile sodium chloride solution 0.9% and sterile heparine solution 25'000 IE/5 ml were purchased from B. Braun AG (Melsungen, Germany). Sterile glucose solution 50% was obtained from Laboratorium Dr. G. Bichsel AG (Unseraen, Switzerland) and DMSO (dimethyl sulfoxide) from Honeywell-Fluka/Fisher Scientific AG (Hampton, USA). Reference material for bioanalysis (efavirenz, D4-efavirenz) was obtained from Toronto Research Chemicals (Toronto, Canada). The marketed formulation of efavirenz used in this paper was Stocrin 50 mg from MSD Merck Sharp & Dohme AG (Kenilworth, United States). Fasted simulated intestinal fluid (FaSSIF) was purchased from Biorelevant.com Ltd (London, UK).

3.2 Methods

3.2.1 Production of Amorphous Solid Dispersions by Hot-Melt Extrusion

ASDs were produced with a ZE HMI 9 mm co-rotating mini twin-screw extruder (Three Tech GmbH, Seon, Switzerland). The five-barrel elements were individually PID-controlled by electrical heating and pressurized air as a coolant. The entry block was cooled by house water circulation assuring a temperature below 25°C. Powders were fed by a flat-bottom double-screw dosing device (Three Tech GmbH). Liquid components were fed through a Model 11 syringe pump (Haward Apparatus, Holliston, USA) through a vertical inlet into the first temperature-controlled block of the extruder (40 mm distal from powder inlet). ***Table 3*** in the supplement contains the extrusion parameters and settings. The extrusion zones' temperatures were chosen below the decomposition temperatres of individual components. Powders for extrusion were blended in a Turbula mixer (Glen Mills Inc., Clifton, USA) or by hand in a mortar depending on the sample size. As no it was not aim to optimize

the mixing and extrusion process, we measured the drug content in all formulations as a quality control and adapted dosings for subsequent experiments. For further analysis, samples were milled using an A 11 basic hand mill (IKA Werke GmBH & Co. KG, Staufen, Germany).

3.2.2 Optimization of Amorphous Solid Dispersions

ASD formulations were prepared by mixing HPMCP, efavirenz and further additives (surfactants or polymers) in different proportions as shown in ***Table 1*** as well as in ***Table 4***, ***Table 5***, and ***Table 6*** of the supplement. In all formulations other than formulation F0, HPMCP HP50 was used (in formulation F0 HPMCP HP55 was used). Produced formulations were analyzed in the following order: In a first step, formulations that were not extrudable into a solid, transparent, and millable extrudate were excluded from further analysis. In a second step, formulations were dissolved in a beaker to match similar conditions (buffer and nominal efavirenz concentrations) as in dissolution tests (section 3.2.3) under continuous stirring with a magnetic stirrer. Formulations, where no substantial dissolution was observed, were excluded from further analysis. Finally, formulations were analyzed in dissolution tests (section 3.2.3) using UV/Vis quantification (section 3.2.4). Best results (***Table 1***) in this test (regarding dissolution rate and extent of supersaturation) were confirmed (section 3.2.3) using HPLC quantification (section 3.2.5) to exclude light dispersion artifacts of colloidal systems.

Table 1 Hydroxypropyl methylcellulose phthalate (HPMCP) based formulations used in the present study. *Theoretical and experimental composition of selected candidates.*

Formulation	Polymer	Added fraction of sucrose palmitate [w/w%]	Added fraction of polysorbate 80 [w/w %]	Nominal drug load [w/w %]	Measured drug load [w/w %]
F0	HPMCP HP55	-	-	20	16.62
F31	HPMCP HP50	10	5	28.9	35.29
F34	HPMCP HP50	10	2.5	29.3	27.32
F36	HPMCP HP50	15	5	27.8	26.01
F37	HPMCP HP50	5	5	30.3	38.40
F38	HPMCP HP50	5	2.5	31.0	33.40
F39	HPMCP HP50	15	10	26.6	28.92
F40	HPMCP HP50	15	2.5	28.3	21.71

3.2.3 Dissolution Testing

The used dissolution system consisted of an AT 7 dissolution tester (Sotax AG, Aesch, Switzerland) set up as paddle apparatus (Ph. Eur. 2.9.3, Apparatus 2 [48]) combined with a CY 7 piston pump (Sotax AG) for automated sampling (UV/VIS only). Glass microfiber filters with a particle retention size of 1 µm were used to filter the samples. The system was controlled by a custom-made dissolution

software (Division of pharmaceutical sciences, University of Basel, version 1.2.0.0). The temperature was set to 37°C and the rotation speed of the paddles was set to 100 rpm. The dissolution medium was 1 liter of 0.05 M phosphate buffer, adjusted to pH 6.8 (according to Ph. Eur. 2.9.3 [48]) or 1 liter of fasted simulated intestinal fluid (FaSSIF) for dissolution in biorelevant buffer. Efavirenz (pure drug, 50 mg/L) was added as powder sieved through a 355 µm sieve to exclude effects of particle size distribution on dissolution tests.

3.2.4 Method of Quantification by UV/Vis

For automated dissolution test sampling, sampling times between 180 s and 240 s and a pumping time of 60 s prior to measurement were chosen. We used a Lambda 25 ultraviolet-visible (UV/Vis) spectrometer with a 1 cm cuvette (PerkinElmer, Waltham, USA) measuring at up to three different wavelengths per sample. This allowed distinction of absorbance of efavirenz (247 nm), additional excipients (271 or 281 nm) and Rayleigh scattering (320, 355 or 380 nm) due to the formation of colloid solutions in the dissolution vessel. We used the following correlation of the Rayleigh scattering at different wavelengths

$$A = \log_{10}\left(\frac{1}{1-c_R\,\lambda^{-4}}\right) \qquad \text{Eq. 1}$$

where A is the absorption, c_R the constant of scattering, and λ the wavelength. We determined c_R by measuring the absorbance at a high wavelength, where no absorption by other ingredients was observed. Eq. 1 then allowed for estimation of Rayleigh scattering at the other wavelengths. Efavirenz release was calculated based on a linear calibration for efavirenz and additional excipients across all measured wavelengths.

3.2.5 Method of Quantification by Chromatography

Samples for HPLC (high performance liquid chromatography) of 1 ml, filtered (0.45 µm PTFE filter by Wicom Germany GmbH, Heppenheim, Germany) and unfiltered, were drawn manually at 4, 8, 16, 32, 64, and 128 min. Samples were prepared for analysis by mixing an aliquot of each sample (500 µL) with pure acetonitrile (500 µL). Reference samples produced by dissolution of known amounts of efavirenz were prepared in the same manner.

The UHPLC system (Shimadzu PLC, Kyoto, Japan) for analysis was equipped with two pumps (LC-30AD), a column oven (CTO-20AC), an autosampler (SIL-30AD), a photodiode array detector (SPD-M30A), and a high sensitivity cell (8 mm). We used a Symmetry C18 4.6 x 100 mm, 3.5 µm column (Waters Corporation, Milford, USA) with an isocratic solvent flow of 1.6 ml/min compose of 50% (v/v) acetonitrile and 50% (v/v) ammonium bicarbonate buffer (containing ammonium bicarbonate and ammonia hydroxide solution 28% (w/v)) adjusted to pH 10. The injection volume was 50 µL. Resulting chromatograms were analyzed using the Lab Solutions software version 5.82 (Shimadzu PLC).

Concentrations were determined by linear calibration from the reference samples. Dissolution results measured by HPLC were normalized to the measured content of efavirenz in the ASDs (refer to section 3.2.6).

3.2.6 Sample Preparation for Content Determination

For content determination, 7 mg of ASD samples were dissolved in 50 ml of phosphate buffer (as in section 3.2.3) and measured by the HPLC method (section 3.2.5).

3.2.7 Animal Studies

We performed animal studies according to Swiss regulations for animal welfare under the license number BS-2836-27529. Rats (Wistar, female, 200-240 g) were jugular vein cannulated and provided by Janvier Labs (Saint-Berthevin Cedex, France). Catheters were daily checked for patency and flushed with 50 µL of a sterile lock solution (250 IU/ml heparin in 50% glucose). Rats were fasted 6 hours prior to the experiments providing water *ad libidum*. The formulation was administered orally by gavage using flexible, FTP 15G gavage tubes of 100 mm length (Instech Laboratories Inc., Plymouth Meeting, USA). The intravenous formulation was administered through the jugular vein catheter. Blood samples of 200 µL blood were drawn through the catheter and the volume was replaced by 200 µL of a sterile heparin-solution (150 IU/ml in 0.9% saline). Samples were collected 5 min before formulation administration as well as 5 min, 15 min, 30 min, 1 h, 1.5 h, 2 h, 3 h, 4 h, 6 h, 8 h, and 24 h (and 48 h for the i.v. formulation) after administration. Food was provided *ad libidum* after the 2 h sample. The lock solution was applied after the 8 h sample. After the last time point, the rats were euthanized using CO_2.

3.2.8 Administered Formulations *In Vivo*

For the i.v. formulation of efavirenz we dissolved 5 mg/kg rat weight efavirenz in a mix of 884 µL/kg PEG 400, 1 ml/kg saline 0.9% and 100 µL/kg DMSO resulting in an application volume of 1.984 ml/kg. We sterilized the formulation by filtering through a 0.22 µm PTFE membrane filter under aseptic conditions. The p.o. formulations of 10 mg/kg were suspended or predissolved (to form drug rich particles) directly before gavage. For details regarding the different formulations, refer to ***Table 7*** in the supplement.

3.2.9 Blood Sample Preparation

The 200 µL of drawn blood was immediately put on 10 µL of a 0.5 M EDTA solution and mixed gently. The anticoagulated blood sample was centrifuged at 4°C at 1000 g for 5 min. Plasma samples were stored at -20°C until analysis.

To prepare samples for mass spectrometry, an aliquot of 20 µL plasma was diluted with 80 µL of methanol containing 250 ng/ml internal standard (D4-efavirenz) to precipitate plasma proteins. The

samples were centrifuged for 30 min at 3000 g and the supernatant was injected directly into the HPLC-MS/MS system.

3.2.10 Bioanalysis and Quantification by Mass Spectrometry

The tandem mass spectrometry (MS/MS) method was adapted from Donzelli et al. [49]. The used HPLC system consisted of two LC-20AD liquid chromatography pumps (Shimadzu PLC, Kyoto, Japan), a Model 7956 column oven (Jones Chromatography Inc., Columbus, USA) and a PAL RTC (CTC Analytics AG, Zwingen, Switzerland) or a SIL-20AC HT autosampler (Shimadzu PLC). An Atlantis C18 2.1 x 50 mm, 3 µm column (Waters Corporation, Milford, USA) was used at a total flow rate of 0.35 ml/min with a binary mixture of methanol containing 0.1% formic acid and water containing 0.1% formic acid using a gradient increasing from 20% to 95% methanol. The injection volume was 5 µl. For specific quantification of efavirenz, we used API 3200 mass spectrometer (AB Sciex, Framingham, USA). ***Table 8*** in the supplement shows detailed parameters.

Reference and quality control samples consisted of Wistar rat plasma (Innovative Research, Novi, USA) spiked with an efavirenz in DMSO solution resulting in different concentrations of efavirenz at a constant content 0.1 % DMSO in the plasma samples. Calibration curves were weighted by $1/x^2$ and a lower limit of quantification of 5 ng/ml was determined through measurement of quality control samples.

3.2.11 Analysis of *In Vivo* Pharmacokinetic Data

The raw data were analyzed by the Microsoft (Redmond, USA) Excel (version 2016) plugin PK Solver by Repka et al. [50] using a non-compartmental model. Derived parameters (area under the curve *AUC*, absolute bioavailability *F*, time of maximal concentration t_{max}, maximal concentration c_{max}) from individual rats were cleared from outliers (Grubbs Test; [51]) and groups were compared in a one-way ANOVA analysis at a 95% confidence interval using a post-analysis Tukey test [52] while testing for equal variance by Levene [53]. Statistical analysis was performed in Origin Pro 2016 Version b9.3.226 (Origin Lab Corporation, Northampton, USA). For the analysis of bioavailability, we normalized for the measured efavirenz content in formulations F0 and predissolved F0.

3.2.12 Cryo-Transmission Electron Microscopy (cryo-TEM)

Samples were prepared by dissolving ASD corresponding to 250 mg/L efavirenz in the same buffer as for dissolution tests (section 3.2.3) under continuous stirring. A 4 µl aliquot of sample was adsorbed onto a holey carbon-coated grid (Lacey, Ted Pella, USA), excess liquid was blotted with Whatman 1 filter paper and vitrified into liquid ethane at -178 °C using a Leica GP plunger (Leica, Austria). Frozen grids were transferred onto a Talos electron microscope (FEI, USA) using a Gatan 626 cryo-holder. Electron micrographs were recorded at an accelerating voltage of 200 kV and a nominal

magnification of 57000 x, using a low-dose system (20 e-/Å^2) and keeping the sample at low temperature.

3.2.13 Mathematical Model of Dissolution and Data Fitting

Dissolution data of formulations were fitted by a piecewise system of ordinary differential equations (ODE) with initial and boundary conditions as follows:

$$\begin{cases} c'(t) = k_{diss}\, c_{solid}(t) + k_{rdiss}\, c_{cris}(t) - k_{cris}\, c(t) \\ c'(t)_{solid} = -k_{diss}\, c_{solid}(t) \\ {c_{cris}}'(t) = k_{cris}\, c(t) - k_{rdiss}\, c_{cris}(t) \\ c_{solid}(0) = d \\ c(0) = 0 \\ c_{cris}(0) = 0 \\ {c'}_{cris}(t < t_c) = 0 \end{cases} \quad \text{Eq. 2}$$

We solved the system of ODEs in Mathematica 11.3 (Wolfram, Oxfordshire, UK). From time *t = 0* until the time of crystallization t_c, only the unidirectional dissolution of drug from the solid ASD compartment (c_{solid}) to dissolved state compartment (*c*) was fitted (rate constant k_{diss}). At times after t_c, drug in the dissolved state recrystallizes to the concentration c_{cris} at rate constant k_{crys} and reversibly at rate constant k_{rdiss}, establishing an equilibrium concentration. Initial conditions for *t = 0* indicate an absence of drug in the dissolved and crystalline states; and a dose *d* is the amount of solid drug in ASD. Boundary conditions for $t = t_c$ were the analytical solutions of the first part of the piecewise function with no drug in the crystalline state. Details on fitting procedures are presented in the supplement (section 9.5).

From resulting fitted functions of filtered dissolution curves, different additional dissolution profile characteristics such as maximal concentration, equilibrium concentration, start and end time of supersaturation, period of supersaturation, area under the curve of supersaturation, the ratio of k_{crys} and k_{rdiss}, and the ratio of maximal concentration and equilibrium concentration were extracted. These characteristics were plotted against the polysorbate 80 content, sucrose palmitate content, the ratio of these two surfactants and the summed content of surfactants in the formulation (scatter matrix). Within the different scatter plots, data points were fitted by linear correlation and the Pearson correlation coefficient was determined.

3.2.14 Physiologically Based Pharmacokinetic Modeling

In order to estimate the *in vivo* dissolution curve of the formulations, we fittet a calibrated PBPK model with respect to the dissolution curve parameters to experimentally obtained pharmacokinetic profiles. We used the open-source PBPK software PK-Sim Version 7.3.0 (Open Systems Pharmacology), with the included standard method for calculation of partition coefficients (PK-Sim standard) and their standard rat model. Fixed model parameters were intestinal solubility (human) and fraction unbound (rat), which were retrieved from literature (***Table 9*** in the supplement). In a

first step, the system was calibrated to i.v. rat data by fitting the parameters plasma clearance, entero-hepatic plasma clearance, permeability, lipophilicity, and specific intestinal permeability (***Table 9*** in the supplement). Starting values were retrieved from PK-Sim calculations, pharmacokinetic analysis, or literature. Except for clearances, a deviation of ± 20% was allowed. In a second step, the p.o. data were fitted with fixed parameter values retrieved from i.v. fitting. Here, the Weibull dissolution parameters dissolution shape and dissolution time [54], as well as the dose, was fitted. From the retrieved Weibull parameters (***Table 10***) and the dose, *in vivo* dissolution curves were plotted. For detailed parameters and references refer to ***Table 9*** and ***Table 10*** in the supplement.

3.2.15 Molecular Dynamics Simulations

Molecular dynamics simulations were carried out using the Desmond molecular dynamics software package 2016.4 (D.E. Shaw Research, New York, USA, [55]) and Maestro 11 (Schrödinger LLC, New York, USA) using the OPLS_2005 definition of the force field. A system composed of 20 reduced length HPMCP HP50 chains (1167 atoms), 104 efavirenz molecules, 39 sucrose palmitate molecules, and 3 polysorbate 80 molecules was created, corresponding to the mass ratios used in Formulation F40 (***Table 1***). Phthalate groups were deprotonated according to the expected ratio at pH 6.8 according to a pK_a of 5.4. The molecules were arranged randomly using PACKMOL version 18 (Universidade Estadual de Campinas, Brazil, [56]). The resulting system and the same system with removed surfactant molecules were each solvated, neutralized by Na^+ ions and molecular dynamics was performed for 20 and 50 ns at body temperature (310,15°K) and atmospheric pressure (scenario I). In addition, the randomly packed systems with and without surfactant molecules were simulated without water molecules for 5 ns to form particles, due to energy minimization. Resulting configurations were solvated, neutralized by Na^+ ions and run again for 20 ns (scenario II). Before each simulation, the system was relaxed by the Desmond standard relaxation protocol and the energy cycle length was 1.2 ps in all simulations. Total systems potential energy, as well as surfaces of the whole molecular ensemble (excluding water and Sodium ions), were recorded

3.2.16 X-Ray Powder Diffraction

To prove the amourphous stat of the produced ASDs, we performed x-ray powder diffraction (XRPD) on a SmartLab diffractometer (Rigaku Corp., Tokyo, Japan) equipped with a 9kW rotating anode generator, Bragg-Brentanto optical geometry and a HyPix-3000 detector. Samples were exposed to radiation (λ = 1.541 Å) from a Cu source and measured in 1D detection mode. For all measurements, a CuK-beta filter was used.

3.2.17 Dynamic Light Scattering

To characterize the size of particles formed upon dissolution of ASDs, dynamic light scattering (DLS) was performed on a Delsa™ Nano (Beckmann Coulter, Brea, USA) with automatically optimized measurement conditions.

4 Results

Hot melt extrudates (ASDs), which were glassy, easy to comminute solids were characterized in more detail (***Table 1***). The added fractions of 5-15% sucrose palmitate and 25-10% of polysorbate 80 did not hinder the milling process of the extrudates (observation), which is very important for further processing of the ground ASDs into tablets. The selected formulations from the (***Table 1***) were investigated for particle morphology, dissolution behavior, and in vivo performance. Information on physical and chemical properties of formulations which did not pass the screening requirements is provided in the supplementary material.

For Formulatoin F0 and F40, additional XRPD analysis was performed (Figure 9). Both formulations did not show any crystallinity peaks as the reference of pure efavirenz. This confirms the amorphous state of the drug in the ASDs.

4.1 Particle Morphology and Molecular Dynamics Simulation

Cryo-TEM imaging of F0 (without surfactants) and F40 (with surfactants) showed particles or aggregates in the submicron to sub millimeter range (***Figure 1***). For formulation F40, DLS measurements showed that 90% of the particles (number distribution) had a average size of 601.6 ± 76.6 nm with a small number of larger aggregates. Particles formed from formulation F0 exposed heterogeneous structure, with irregular shapes and surfaces. Particles formed from formulation F40 were coalescing into random pattern aggregates and showed smooth surfaces. Time-resolved imaging of formulation F40 at different time points after the beginning of dissolution demonstrated an overall tendency of smaller particles to form larger clusters after 2 hours. After 5 hours, drug crystals appeared in the samples, which suggests particle decomposition and the crystallization of the API, as seen in Figure 1,e withcrystalline needles. It can be speculated that mainly the hydrophilic core undergoes decomposition with subsequent release and recrystallization of drug.

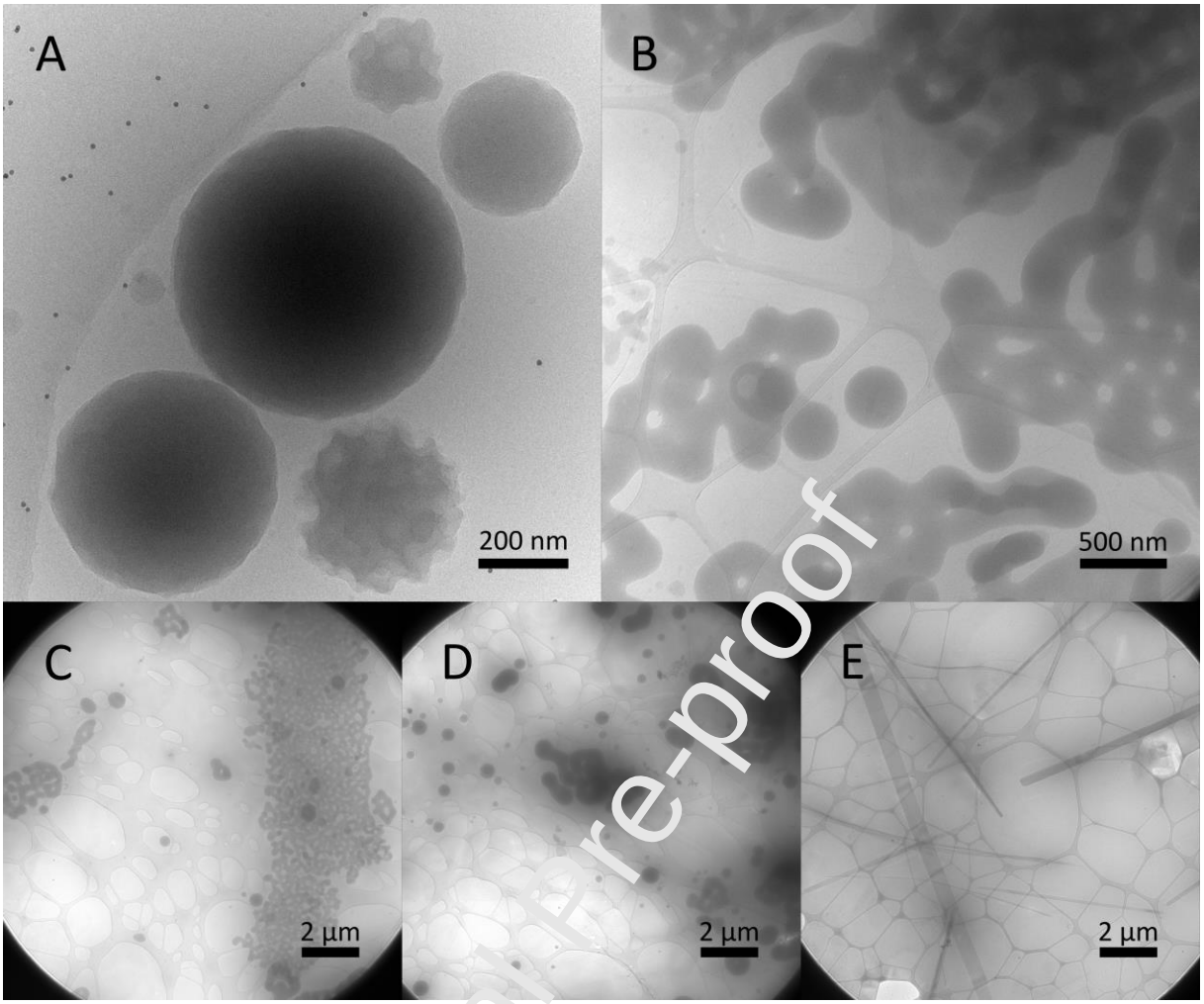

Figure 1: Cryo-TEM images of formulation F0 and formulation F40. *Formulations F0 (A) and F40 (B) were analyzed by cryogenic electron microscopy. Changes in formulation F40 over time were monitored at 30 min (C), 2 h (D) and 5 h (E) after start of dissolution.*

Results of molecular dynamics simulations (***Figure 2***) showed that in scenario I, an entanglement of molecules was simulated while in scenario II a disentanglement of the molecules was obtained (***Figure 2 B***). The analysis of surfaces around the molecular ensemble of simulated molecules (excluding water) supported these results (***Table 11*** in the supplement).

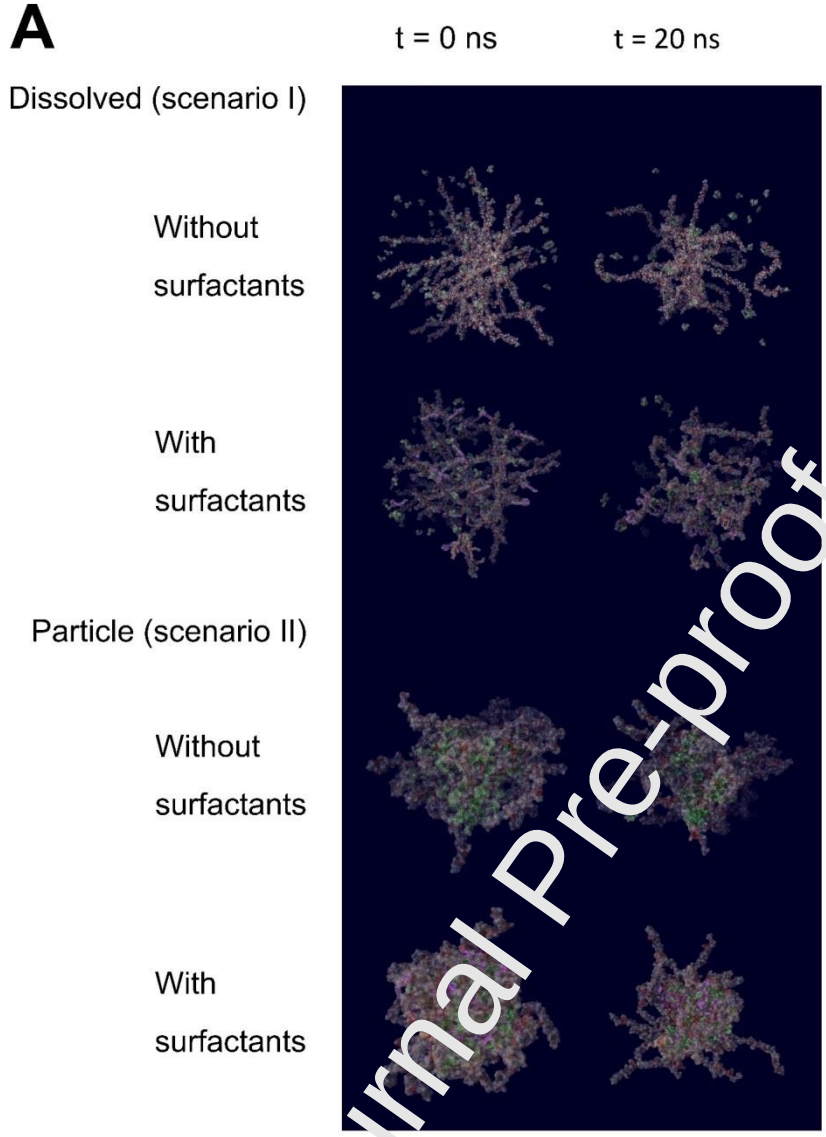

Figure 2: Molecular dynamic simulation of particle morphology. *Different starting conditions were defined for the simulations: In scenario I, molecules were arranged randomly and solvated. In scenario II, molecules were first condensed into particles and then solvated. Both scenarios were carried out with and without surfactants (sucrose palmitate and polylobate 80).* ***A*** *Molecular ensemble states at times 0 and 20 ns. Efavirenz is colored green, sucrose palmitate pink, polysorbate 80 orange and polymers gray. A semi-transparent surface was created around the included molecules to visualize electric potentials. Water molecules are not displayed for better visibility.*

4.2 Results of *In Vitro* Testing and Modeling

The performance of the the formulation were mostly assessed with dissolution tests using phosphate buffer. While the addition of water-soluble polymers in formulations F1-11 (***Table 4*** in supplement) did not impact dissolution (data not shown), the addition of surfactants has improved the dissolution properties (***Table 1***, ***Table 5*** in the supplement). In our case, adding water-soluble polymers to the

ASD seemed to be a promising strategy to improve ASD performance and therefore was not further investigated. The best surfactant combination was identified as a mixture of sucrose palmitate and polysorbate 80. An optimization screening to identify the optimal content of the excipients with respect to enhance dissolution performance resulted in a formulation containing 15% (w/w) of sucrose palmitate and 2.5% (w/w) of polysorbate 80 (formulation F40, ***Table 1***). This compositionshowed a complete drug release within first 16 min of dissolution. The formulation without surfactants F0 released only 55% (w/w) of drug during the first 16 minutes and the marketed formulation yields only 30% drug release at the same time point. Decrease of drug concentrations in filtered fractions, especially in formulations with surfactants, suggests drug precipitation from the supersaturated solution. In contrast, and as expected, the marketed formulation did not show any effect of supersaturation (***Figure 3***). The ground particles of formulation F0 (without surfactant) dissolved incompletely and ASD-particles turned white, hinting on recrystallization of efavirenz on the surface of the particles, as described in the literature [57,58]. In contrast to F0, formulation F40 (with surfactant) showed complete dissolution and the formation of a colloidal solution.

Aiming to achieve better comparability between *in vitro* and *in vivo* results, formulations F0 and F40 were also tested in biorelevant medium (FaSSIF). Results showed fast and complete release profiles for both formulations (**Figure 3**)..

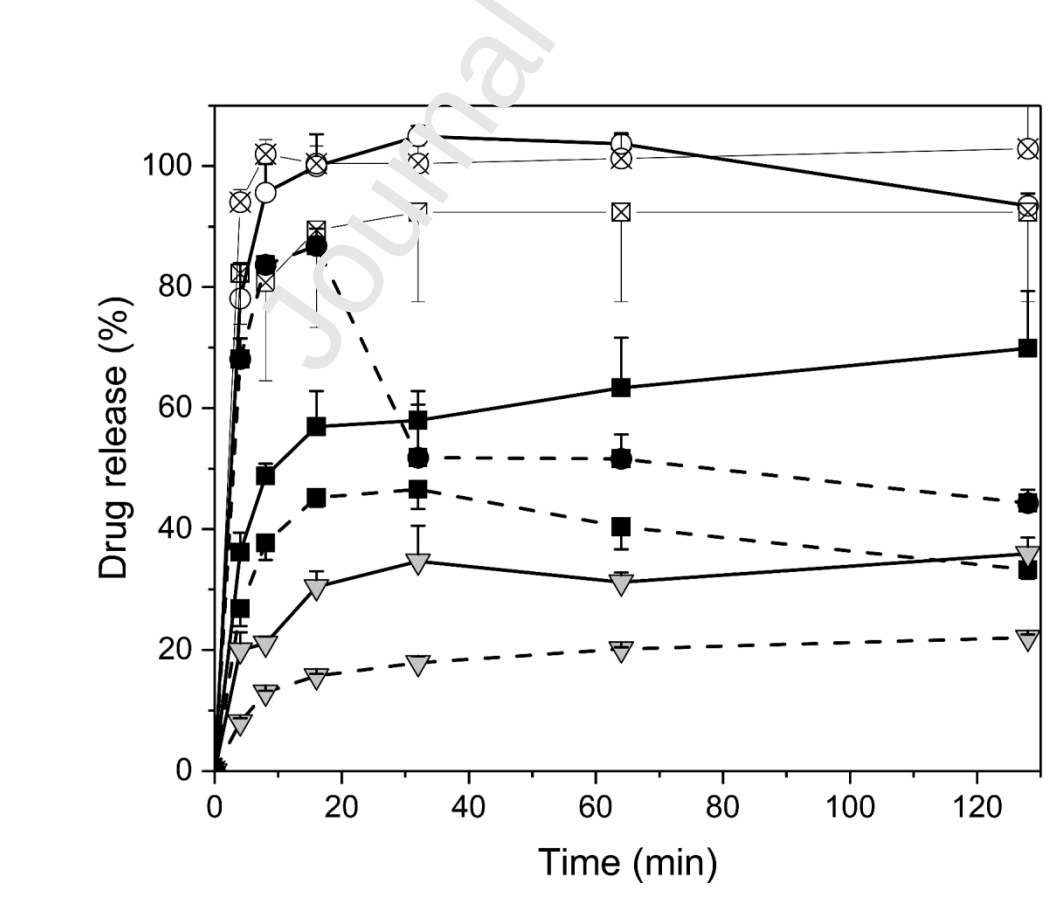

Figure 3: Dissolution profiles. *Dissolution of formulation F0 (without surfactants, black squares), formulation F40 (with surfactants, white circles) and the marketed formulation (gray triangles). Empty crossed squares and circles connected with thin lines are formulations F0 and F40 in FaSSIF, respectively. Values are means ± S.D., n=3. Solid lines depict the unfiltered fraction and dashed lines the filtered fraction.*

Table 2 summarizes findings from correlation analysis between dissolution profile characteristics and formulation content properties. Higher total surfactant and sucrose palmitate content have a positive impact on equilibrium concentrations (c_{eq}). Furthermore, higher total surfactant and polysorbate 80 content delay dissolution and recrystallization. It should be noted that surfactants had an impact on equilibrium concentrations (c_{eq}) but no on maximal concentrations measure during dissolution (c_{max}).

Table 2: Correlation between dissolution profile characteristics and formulation content properties. *Summary of observed correlations for filtered fractions with Pearson correlation coefficient r > 0.7 or r < - 0.7. Formulation parameters: the content of total surfactant or content of polymer (polysorbate 80 or sucrose palmitate). Dissolution profile characteristics: Dissolution rate constant k_{diss}, time of crystallization onset t_c, time to supersaturation onset t_{sup}, and concentration at equilibrium state c_{eq}. Tested concentration ranges: see **Table 1**, Formulations F31, F34, and F36-F40.*

Dissolution profile characteristics	Formulation Parameter	Pearson correlation coefficient
c_{eq}	Total surfactant	0.896
t_c	Total surfactant	0.749
t_{sup}	Total surfactant	0.835
t_c	Polysorbate 80	0.853
t_{sup}	Polysorbate 80	0.863
c_{eq}	Sucrose palmitate	0.964

4.3 Results of *In Vivo* Testing and Modeling

Comparable bioavailabilities were observed for the marketed formulation and the physical mixture of polymer of formulation F0 and efavirenz (***Figure 4***). The corresponding extruded formulation F0 showed only a marginal bioavailability, while the predissolved formulation F0 had the highest bioavailability among others. Surfactants in F40 increased the bioavailability compared to the ASD without surfactants (F0). Regarding the time necessary to reach the maximum concentration in plasma, the marketed formulation had the shortest t_{max}, whereas the physical mixture had an increased t_{max}. The predissolved formulation F0 and the marketed formulation yielded highest c_{max} in rat plasma (supplement ***Figure 8***).

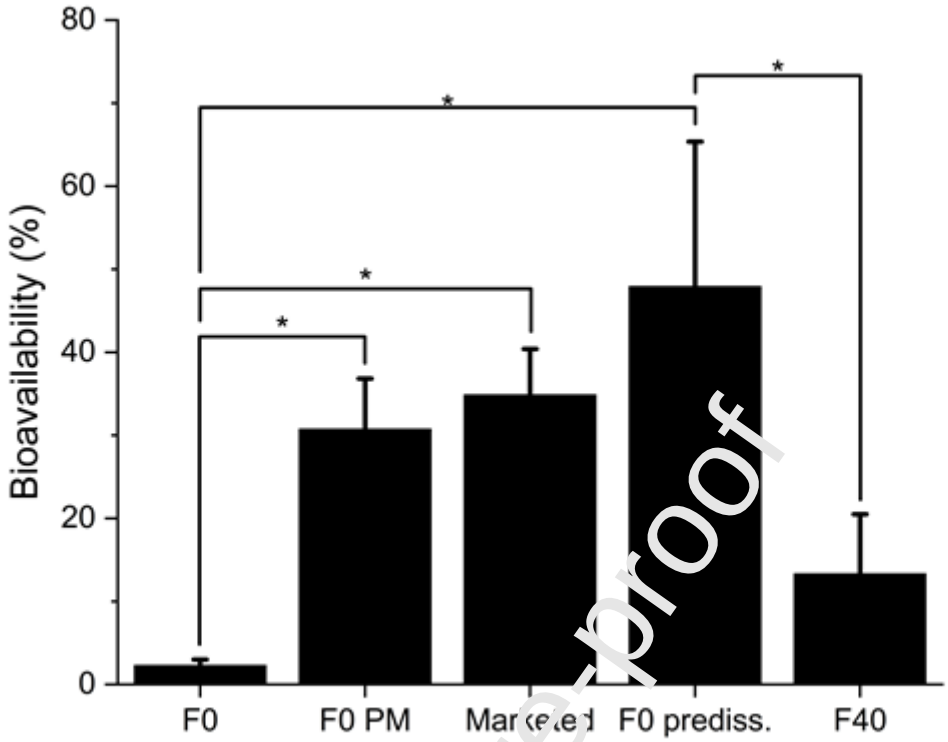

Figure 4: Oral bioavailability (24 h) of efavirenz formulations. *Comparison of formulation F0 (n=2), physical mixture of efavirenz and polymer of formulation F0 (F0 PM; n=3), marketed formulation (n=3), predissolved formulation F0 (F0 prediss.; n=3), and formulation F40 (n=4). Values are means ± S.D, statistical analysis was done at a significance level of 0.05.*

The results of the deconvolution of the fitted pharmacokinetic data with the PBPK model (calculated *in vivo* dissolution curves) suggest an incomplete release in all formulations (***Figure 5***). While the predissolved formulation F0 showed a maximal *in vivo* release of approximately 50%, the physical mixture of formulation F0 and the marketed formulation showed a maximum at approximately 25%. Formulation F40 liberated only approximately 5% of the drug substance and the ASD formulation F0 showed a release close to zero. With respect to the relative dissolution speed, the dissolved formulation F0 and formulation F40 showed the fastest release. The physical mixture of formulation F0 and the marketed formulation both showed moderate and comparable dissolution rates.

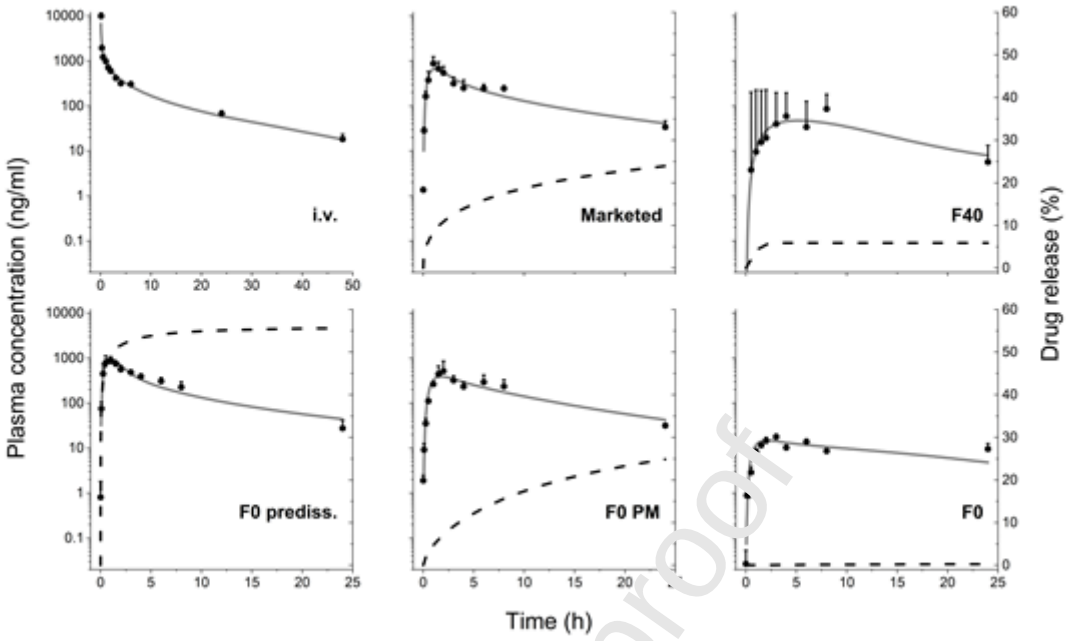

Figure 5: Plasma concentration-time curve and simulated drug release in rats with simulated in vivo dissolution profiles. *Primary y-axis, solid line: Fitted plasma concentrations after i.v. efavirenz solution (5 mg/kg, n=3) or p.o. administration (10 mg/kg) of efavirenz in form of the marketed formulation (n=3), formulation F40 (n=3), predissolved formulation F0 (F0 prediss., n=3), physical mixture of formulation F0 (PM, n=3), and formulation F0 (n=2). Secondary y-axis, dashed line: Simulated in vivo drug release. Values are means ± S.D.*

5 Discussion

As outlined in the introduction, ASDs are promising formulations to increase bioavailability. However, the mechanisms of dissolution, in-situ formation of drug-rich carrier vesicles and in vivo bioavailability are poorly understood. As the physiologically relevant drug delivery system, i.e. drug-rich particles formed upon dissolution, is formed *in situ*, it is of great interest to control and fine-tune the behavior of the system, e.g., by additional excipients such as surfactants. In addition, the influence of such excipients on the vesicle formation mechanism is not entirely understood, making the rational design of ASD-based medicine difficult yet. In this study, we provide insights into the in-situ formation of the carrier vesicles and the influence of surfactant on uptake mechanisms from amorphous solid dispersions. To elucidate these mechanisms, the used modeling methods (molecular dynamics, dissolution data fitting, and physiologically based pharmacokinetic modeling) proved to deliver valuable information beyond the mere experimental results.

We chose the model system of efavirenz as model drug and HPMCP as base polymer. The surfactants sucrose palmitate and polysorbate 80 were chosen based on dissolution experiments. ***Figure 6*** depicts the insight gained from this study. *In vitro*, the ASD formulation containing only HPMCP as polymer (without surfactants) forms particles during dissolution and leads to supersaturation compared to the marketed formulation, supporting the suitability of this polymer for use in ASDs (***Figure 6***, A). However, the dissolution of such ADSs was incomplete. By adding a suitable ratio of selected surfactants, supersaturation is maximized and a complete dissolution is achieved. The two surfactants seem to influence the dissolution curve independently: While sucrose palmitate increased the supersaturated equilibrium concentration, polysorbate 80 increased the time to supersaturation and prolonged the time to recrystallization (***Figure 6***, C). *In vivo*, ASDs without surfactants showed a marginal dissolution. However, once drug-rich particles formed (i.e. externally predissolved ASDs), an efficient uptake of drug from the particles was observed, proving the validity of the drug-rich particles for oral drug delivery (***Figure 6***, B). With surfactants, an increased overall bioavailability was observed (***Figure 6***, D), however no extended animals study was performed as a corresponding study is aimed to be performed in humans (clinical trial registered under NCT03886766).

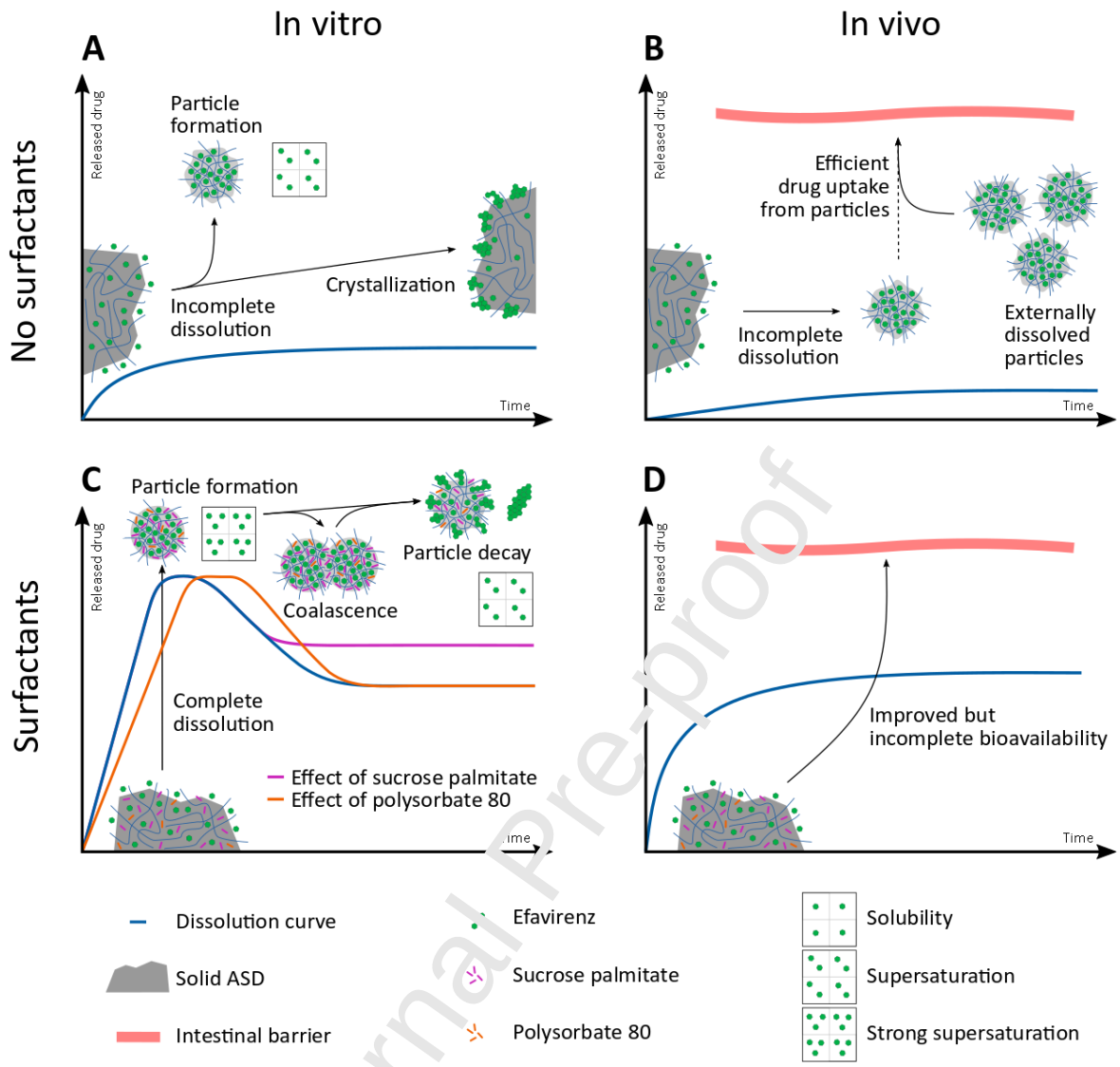

Figure 6: Schematic illustration of the dissolution of and particle formation from ASDs*. Description of in vitro and in vivo insights based on the impact of surfactants.*

From a conceptual point of view, complete and fast dissolution from ASD into drug-rich particles is a crucial first step in the cascade to systemic drug uptake. The detailed mechanisms of the formation of drug-rich particles from ASDs (e.g. driven by a temporary dissolution of individual ASD compounds or the disintegration of particles directly from the ASD) was not investigated in this study. *In vitro*, we showed that surfactants clearly promote this step. In addition, *in vitro* behavior was responsive to changes of the ratios of the two surfactants (***Figure 6***, C). In the second step in the cascade to systemic drug uptake, the drug needs to be absorbed from the drug-rich particles. In contrast to the localization of poorly soluble drugs in micelles, which can have a negative effect on the flow through the intestinal membrane [59], drug-carrier particles emerging from ASDs are proposed not to hinder the flux[60,61] (***Figure 6***, B). This is in line with the hypothesis that drug-rich particles formed by ASDs represent a reservoir, from which API can diffuse rapidly into solution for subsequent intestinal

absorption [18]. In this study, the function of the drug-rich particle as such a reservoir was shown *in vivo* for the formulation without surfactants (***Figure 6***, B). For the formulation with surfactants, an increased bioavailability was observed (***Figure 6***, D).

5.1 Effect of Surfactants on Particle Morphology

The obersved particles size in cryo-TEM was in line with the particle size characterization by DLS. The addition of surfactants to the formulation seems to facilitate particle formation. Surfactants also influenced particle-particle interactions. While in the absence of surfactants, particles were observed strictly individually, there was a frequent interaction between the particles observed in the presence of surfactants (***Figure 6***, C). This might have different reasons: 1) Looking at the complex structures observed, it could also be hypothesized that the particles or aggregates had a low surface energy, allowing for a transitional phase of a non-beneficial surface to volume ratio, therefore facilitating formation of dispersions;2) surfactants on the surface of the particles enable interparticle interaction due to similar hydrophobicity of the surface groups; and 3) surfactants induced the formation of different particles, based on different physicochemical principles (e.g. LLPS vs. micelles). Even though the coalescence of particles over time into larger particles is likely (see below), it is also possible that smaller particles also emerge from large particles or from the surface of an ASD particle due to applied shear forces.

As can be seen in ***Figure 1 C-E***, the particles were not stable over time: Particles increased in size and had disappeared after 5 hours, which triggered the recrystallization of efavirenz. This is in line with the dissolution results (refer to section 4.2), where the concentration in the filtered fraction decrease. These insights (***Figure 6***, C) are important to estimate a time-limited stability and assures the release of efavirenz and consequently, its availability for uptake from the intestinal lumen.

The spontaneous molecular arrangement of ASD compounds into drug-rich particles was confirmed by MD simulations. When performing MD simulations starting with individually dissolved ASD components (scenario I), the formation of a particle was observed after 20ns. More pronounced results were obtained for a longer, i.e., 50 ns simulations. At the same time, when starting with a preformed ASD particle separated from the surrounding water, a decompositoin of the particle could be observed. This indicates that 1) the optimal state can be described as an intermediate state between individually dissolved ASD components and complete segregation of ASD compounds from water. Furthermore 2), it can be expected that the particles form spontaneously form dissolved ASD compounds but also allow for a liberation of the compounds from a complete segregated state (e.g. the solid ASD). The change of the surface area of the molecular ensembles (excluding water) is in line with this observation. Differences between the systems with or without surfactants could be explained by the low solubility of sucrose palmitate, which facilitates the aggregation of molecules

and inhibits particle hydration. These insights are supported by the recorded molecular trajectories during simulation. Sucrose palmitate, together with efavirenz, seems to localize in the middle of the ensemble of molecules, creating a hydrophobic core, while the polymer chains seem to orient towards the water. These cores might also be responsible for the higher equilibrium concentration correlating to the content of sucrose palmitate during the dissolution test. A higher content of the hydrophobic sucrose palmitate in the ASD could contribute to the formation of hydrophobic cores, creating a larger volume stabilization matrix, where higher concentrations of amorphous efavirenz is possible (***Figure 6***, C). Sucrose palmitate could therefore be ascribed a solubilizing role. In contrast, in the system without surfactants, efavirenz alone seems not to localize in a core within the polymer chains. This could be explained by an insufficient amount of hydrophobic moieties.

Looking at the role of the polymer, it is interesting to observe that efavirenz seems to aggregate with the parts of the polymer chains that are not charged, i.e. in sections without phthalates. The polymer itself therefore might also have a solubilizing effect, which could explain the comparably good results of the physical mixture's bioavailability *in vivo*. Furthermore, for the formation of stable particles, it seems crucial that the polymer can interact with all molecules in the ASD as well as in water. From this observation, it can be assumed that the polymer plays an important role in bridging the interaction of water and further excipients.

Based on MD observations, Polysorbate 80 seems to have similar action as sucrose palmitate, however, due to the low number of polysorbate 80 molecules that could be included in the MD simulation due to computational limitations, no conclusion on its function can be made based on these results.

The molecular dynamics simulations, has besides its opportunities also limitations, e.g. that the time scale of simulation is not comparable to experimental time scales and complete convergence of the system was not possible. Furthermore, the effect of pH, which we accounted for by a static deprotonation of phthalate groups in the HPMCP chains, hinders the formation of local differences of pH and therefore degree of deprotonation. Less deprotonation for example would be expected in the core of the particle, where water molecules are rare and the environment is mostly hydrophobic. Furthermore, long calculation times of such large systems limits the number of simulations at hand, which is also why no statistical model discrimination tests were performed.

5.2 Effects of Surfactants *In Vitro*

The fitting of the experimentally obtained dissolution curves with the established mathematical model allows for the description of the different sub-processes occurring at the same time (dissolution of ASDs, crystallization and redissolution). Especially for systems where supersaturation is dynamic and unstable, this method could be valuable alternative to static solubility or

supersaturation measurements, which both are not always possible to perform experimentally and might be of limited use for the characterization of the dynamic situation *in vivo*.

Considering the observations of surface recrystallization made during dissolution testing (section 4.2), it can be hypothesized that the addition of surfactants can suppress drug recrystallization of efavirenz during dissolution, as was reported for other combinations of drugs and surfactants [62-64]. Even though partial dissolution and particle formation were also observed in formulation F0 without surfactants, it could be assumed that in absence of surfactants polymer and drug did not dissolve congruently. Therefore, the composition of the formed particles is, probably, not the same as of the ASD [17]. This could eventually lead to a surplus of drug that is no longer stabilized in its amorphous form by the polymer, which results in recrystallization. In addition, surfactants aid in maintenance of a temporary supersaturation.

Looking at the role of the individual surfactants on dissolution behaviour, it is interesting to note that there were no correlations found between dissolution profile characteristics (section 3.2.13) and the ratio of the sucrose palmitate and polysorbate 80. We hypothesize that the two surfactants independently enhance dissolution properties based on different mechanisms (***Figure 6***, C). This could allow for specific control of the formulation behavior by choosing specific surfactant contents in the ASD. The independency is underlined when looking at the identified correlations. The strongest correlation was found between the content of sucrose palmitate and the equilibrium concentration c_{eq}. It therefore can be hypothesized that sucrose palmitate is essential to stabilize efavirenz in the form of drug-rich particles in this equilibrium. Polysorbate 80 was found to increase time to re-crystallization t_c, therefore prolonging drug solubilization. In addition, polysorbate 80 increases the time to supersaturation t_{sup}. As there was no significant correlation with the area under the curve of supersaturation and polysorbate 80, its effect on total dissolved drug exposure might not be significant. Correlations of the total amount of surfactants are in line with the corresponding individual. The absence of a correlation of total surfactants and c_{max} demonstrates that surfactants mainly influence the equilibrium concentration and not the maximal concentration.

5.3 It can be hypothesized that sucrose palmitate mainly influences the equilibrium concentration c_{eq}, while polysorbate 80 instead influences the dissolution kinetics of the system (*Figure 6*, C). With respect to physicochemical properties of the two surfactants, polysorbate 80 is well soluble in water (100 mg/ml) with a hydrophilic-lipophilic balance (HLB) value of 15 [65], while sucrose palmitate is much less soluble in water (poorly soluble) [66] having the same HLB value of 15 [67]. From the difference in solubility it could be assumed, that sucrose palmitate has a higher affinity to efavirenz and therefore might be the first interaction partner. This could explain the stabilizing effects of sucrose palmitate on the equilibrium concentration. In contrast, polysorbate 80 is more likely to interact also with water, therefore enabling but also controlling dissolution kinetics and drug-rich particle stability. While we can hypothesize on the physicochemical nature for the observed impact on dissolution behavior by the surfactants, more detailed studies would be necessary to prove these ideas experimentally.The comparison of formulation F0 and F40 in dissolution testing with biorelevant media showed comparable release profiles for both formulations, indicating a sufficient increase in the solubility of the drug in presence of bile salts to maintain sink conditions. Despite the use of biorelevant media helps to predict the *in vivo* behavior from *in vitro* results in some cases, the use of non-sink conditions allows for a better observation of supersaturation phenomena. Acid-buffer stage dissolution experiments were not performed, as due to the poor solubility of the polymer at low pH. Effect of Surfactants *In Vivo*

Bioavailability studies in rats delivered contrary results than expected from *in vitro* experiments. Especially formulation F0 showed only a marginal absorption of efavirenz into the systemic circulation (***Figure 6***, B). The addition of surfactants enhanced bioavailability even at higher drug loading, however, did not reach the level of the physical mixture (formulation F0) and the marketed formulation. Besides the effect of the surfactants, also the slightly different base polymers (HPCMP HP50 in formulation F40 in contrast to HP55 in Formulation F0), could have improved the performance of the formulation as with HPMCP HP50 already dissolves at a lower pH. However, as the two polymers dissolve at pH of 5.0 (HPMCP HP50) or pH 5.5 (HPMCP HP55) [29,30], i.e., at pH-values lower than those in dissolution tests or as it would be expected in the intestine, the impact of this difference in polymer structures is estimated as negligible.

More detailed analysis of pharmacokinetic results by PBPK parameter identification was performed to simulate *in vivo* dissolution based the measured pharmacokinetics. This analysis gives more information on the critical, dynamic dissolution step *in vivo* compared to standard pharmacokinetic analysis of static parameters such as relative bioavailability, t_{max}, or c_{max}. At the same time, it is important to mention, that these dissolution curves are an indirect simulations based on a complex model, where risk of a significant error is high. As expected, the predissolved formulation F0 showed

the fastest simulated *in vivo* release, indicating fast initial uptake form drug-rich particles. The physical mix of formulation F0 and the marketed formulation yielded similar results, with a slightly faster release of the marketed formulation, probably due to sodium lauryl sulfate in the formulation. An addition of surfactants (in the formulation F40 compared to formulation F0) resulted in a manifold release, however still incomplete (***Figure 6***, D). It is interesting to note, that release from formulation F40 was initially fast, but then levelled off in an early stage. A possible reason could be recrystallization of efavirenz, as is was observed *in vitro* for formulation F0.

Comparing our results with the literature*, in vivo* results are in line with the results of Miao et al. [27]: Using a comparable polymer (hydroxypropyl methylcellulose acetate succinate, HPMCP-AS), no favorable effect on bioavailability was measured in *in vivo* in contrast to the expected positive effect based on *in vitro* results. In this study, the favorable bioavailability also measured for the predissolved formulation F0 indicates that the dissolution step from solid ASD to the drug-rich particles might be the critical step in the cascade of *in vivo* bioavailability. The uptake of drug from the drug-rich particles seems not to be the limiting factor. This validates the possibility of drug delivery by the observed particles, provided that where *in vivo* dissolution is sufficiently fast. Furthermore, Frank et al. [20], showed that a similar combination of surfactants was identified as favorable, despite using a different polymer (PVP/VA 64) and API (ABT-102). It might be worthwhile to investigate if the combination of these surfactants could act as a solubility enhancer for other base polymers and other APIs. As *in vivo* results were controversial to this *in vitro* finding, more research will be needed to estimate the potential of HPMCP, also in combinations with surfactants, for use in ASD.

Bioavailability experiments in rats can show valuable within-species difference between formulations and are a useful extension of *in vitro* methods. However, a direct correlation in animal and human bioavailability is not given [68,69], also due to physiological differences in pH, volumes, transition times, etc. [70–74]. A study in humans using sub-therapeutic doses of formulation F40 was approved by Swiss authorities and will be conducted to elucidate the behavior of the formulation directly in humans (clinical trial registered under NCT03886766). Before having human data, it remains an open question if the promising *in vitro* results or the unfavorable *in vivo* results will be more predictive for formulations design in humans.

6 Conclusion

It was possible to produce amorphous solid dispersions (ASD) using HPMCP as a base polymer and to effect *in vitro* and *in vivo* performance of the ASD by the addition of the surfactants sucrose palmitate and polysorbate 80. *In vitro* results indicated an improvement of the dissolution compared

to pure efavirenz or the marketed formulation and showed effects on the drug-rich particle formed *in situ* upon dissolution. Based on mechanistic analysis, we hypothesize that the two surfactants serve independent purposes with respect to the dissolution profile. *In vivo* results (rats) support a positive effect of the addition of surfactants on the performance of the formulation has been shown. Results of *in vivo* analysis indicated that limiting step in bioavailability seems to be the formation of particles in the intestinal lumen from the ASD. Hindrance of drug absorption from the formed particles was not detected.

Methods like mathematical modeling of dissolution data, molecular dynamics (MD) simulations, physiologically based pharmacokinetic modeling (PBPK) and cryo-TEM imaging can deliver valuable insights into complex mechanisms that govern dissolution, the formation of drug-rich particles, and *in vivo* behavior of ASDs. Based on the results in this study, we hypothesize that surfactants can be used to fine-tune the dissolution behavior and particle formation from ASDs and therefore further enhance bioavailability. Further mechanistic investigations *in vitro*, *in vivo* and in humans are necessary to strengthen these insights, prove our hypothesis in sufficient details, and to further advance ASD as drug delivery platform for poorly soluble drug substances, especially with respect to admixed surfactants

7 Acknowledgment

We are grateful to Prof. Dr. Stephan Krähenbühl for his continuous support and would like to thank Dr. Urs Duthaler for his help concerning the mass spectrometry measurements. We would like to thank Carola Alampi and Mohamed Chami from the BioEM Lab at Center for Cellular Imaging and NanoAnalytics (C-CINA) at the University of Basel at the Department for Biosystems Science and Engineering (D-BSSE).

8 References

[1] R. Lipp, The Innovator Pipeline: Bioavailability Challenges and Advanced Oral Drug Delivery Opportunities, 16 (2013). http://www.americanpharmaceuticalreview.com/Featured-Articles/135982-The-Innovator-Pipeline-Bioavailability-Challenges-and-Advanced-Oral-Drug-Delivery-Opportunities/ (accessed April 4, 2019).

[2] M.J. Waring, J. Arrowsmith, A.R. Leach, P.D. Leeson, S. Mandrell, R.M. Owen, G. Pairaudeau, W.D. Pennie, S.D. Pickett, J. Wang, O. Wallace, A. Weir, An analysis of the attrition of drug candidates from four major pharmaceutical companies, Nat. Rev. Drug Discov. 14 (2015) 475–486. doi:10.1038/nrd4609.

[3] Padden et al., Amorphous Solid Dispersions as Enabling Formulations for Discovery and Early Development, (2011). http://www.americanpharmaceuticalreview.com/Featured-Articles/37035-Amorphous-Solid-Dispersions-as-Enabling-Formulations-for-Discovery-and-Early-Development/ (accessed March 28, 2019).

[4] Y. Huang, W.-G. Dai, Fundamental aspects of solid dispersion technology for poorly soluble drugs, Acta Pharm. Sin. B. 4 (2014) 18–25. doi:10.1016/j.apsb.2013.11.001.

[5] S.Y.K. Fong, A. Bauer-Brandl, M. Brandl, Oral bioavailability enhancement through supersaturation: an update and meta-analysis, Expert Opin. Drug Deliv. 14 (2017) 403–426. doi:10.1080/17425247.2016.1218465.

[6] Sharma A., Jain C.P., Solid dispersion: A promising technique to enhance solubility of poorly water soluble drug, Int. J. Drug Deliv. 1 (2011) 149–170.

[7] A. Haser, F. Zhang, New Strategies for Improving the Development and Performance of Amorphous Solid Dispersions, AAPS PharmSciTech. (2018) 1–13. doi:10.1208/s12249-018-0953-z.

[8] M.M. Crowley, F. Zhang, M.A. Repka, S. Thumma, S.B. Upadhye, S.K. Battu, J.W. McGinity, C. Martin, Pharmaceutical Applications of Hot-Melt Extrusion: Part I, Drug Dev. Ind. Pharm. 33 (2007) 909–926. doi:10.1080/03639040701498759.

[9] M.A. Repka, S.K. Battu, S.B. Upadhye, S. Thumma, M.M. Crowley, F. Zhang, C. Martin, J.W. McGinity, Pharmaceutical Applications of Hot-Melt Extrusion: Part II, Drug Dev. Ind. Pharm. 33 (2007) 1043–1057. doi:10.1080/03639040701525627.

[10] S. Baghel, H. Cathcart, N.J. O'Reilly, Polymeric Amorphous Solid Dispersions: A Review of Amorphization, Crystallization, Stabilization, Solid-State Characterization, and Aqueous Solubilization of Biopharmaceutical Classification System Class II Drugs, J. Pharm. Sci. 105 (2016) 2527–2544. doi:10.1016/j.xphs.2015.10.008.

[11] S. Baghel, H. Cathcart, N.J. O'Reilly, Understanding the generation and maintenance of supersaturation during the dissolution of amorphous solid dispersions using modulated DSC and 1H NMR, Int. J. Pharm. 536 (2018) 414–425. doi:10.1016/j.ijpharm.2017.11.056.

[12] K. Ueda, K. Higashi, M. Kataoka, S. Yamashita, K. Yamamoto, K. Moribe, Inhibition mechanism of hydroxypropyl methylcellulose acetate succinate on drug crystallization in gastrointestinal fluid and drug permeability from a supersaturated solution, Eur. J. Pharm. Sci. 62 (2014) 293–300. doi:10.1016/j.ejps.2014.06.007.

[13] K. Ueda, K. Higashi, K. Moribe, Mechanistic elucidation of formation of drug-rich amorphous nanodroplets by dissolution of the solid dispersion formulation, Int. J. Pharm. 561 (2019) 82–92. doi:10.1016/j.ijpharm.2019.02.034.

[14] K. Ueda, K. Higashi, K. Moribe, Direct NMR Monitoring of Phase Separation Behavior of Highly Supersaturated Nifedipine Solution Stabilized with Hypromellose Derivatives, Mol. Pharm. 14 (2017) 2314–2322. doi:10.1021/acs.molpharmaceut.7b00178.

[15] A.S. Indulkar, J.E. Waters, H. Mo, Y. Gao, S.A. Raina, G.G.Z. Zhang, L.S. Taylor, Origin of Nanodroplet Formation Upon Dissolution of an Amorphous Solid Dispersion: A Mechanistic Isotope Scrambling Study, J. Pharm. Sci. 106 (2017) 1998–2008. doi:10.1016/j.xphs.2017.04.015.

[16] G.A. Ilevbare, L.S. Taylor, Liquid–Liquid Phase Separation in Highly Supersaturated Aqueous Solutions of Poorly Water-Soluble Drugs: Implications for Solubility Enhancing Formulations, (2013). doi:10.1021/cg301679h.

[17] S. Saboo, N.A. Mugheirbi, D.Y. Zemlyanov, U.S. Kestur, L.S. Taylor, Congruent release of drug and polymer: A "sweet spot" in the dissolution of amorphous solid dispersions, J. Controlled Release. 298 (2019) 68–82. doi:10.1016/j.jconrel.2019.01.039.

[18] A.S. Indulkar, Y. Gao, S.A. Raina, G.G.Z. Zhang, L.S. Taylor, Exploiting the Phenomenon of Liquid–Liquid Phase Separation for Enhanced and Sustained Membrane Transport of a Poorly Water-Soluble Drug, Mol. Pharm. 13 (2016) 2059–2069. doi:10.1021/acs.molpharmaceut.6b00202.

[19] L.I. Mosquera-Giraldo, N. Li, V.R. Wilson, B.L.B. Nichols, K.J. Edgar, L.S. Taylor, Influence of Polymer and Drug Loading on the Release Profile and Membrane Transport of Telaprevir, Mol. Pharm. 15 (2018) 1700–1713. doi:10.1021/acs.molpharmaceut.8b00104.

[20] K.J. Frank, U. Westedt, K.M. Rosenblatt, P. Hölig, J. Rosenberg, M. Mägerlein, G. Fricker, M. Brandl, The amorphous solid dispersion of the poorly soluble ABT-102 forms nano/microparticulate structures in aqueous medium: impact on solubility, Int. J. Nanomedicine. 7 (2012) 5757–5768. doi:10.2147/IJN.S36571.

[21] J. Kanzer, S. Hupfeld, T. Vasskog, I. Tho, P. Hölig, M. Mägerlein, G. Fricker, M. Brandl, In situ formation of nanoparticles upon dispersion of melt extrudate formulations in aqueous medium

assessed by asymmetrical flow field-flow fractionation, J. Pharm. Biomed. Anal. 53 (2010) 359–365. doi:10.1016/j.jpba.2010.04.012.

[22] K. Ueda, K. Higashi, W. Limwikrant, S. Sekine, T. Horie, K. Yamamoto, K. Moribe, Mechanistic Differences in Permeation Behavior of Supersaturated and Solubilized Solutions of Carbamazepine Revealed by Nuclear Magnetic Resonance Measurements, Mol. Pharm. 9 (2012) 3023–3033. doi:10.1021/mp300083e.

[23] A.-C. Jacobsen, P.A. Elvang, A. Bauer-Brandl, M. Brandl, A dynamic in vitro permeation study on solid mono- and diacyl-phospholipid dispersions of celecoxib, Eur. J. Pharm. Sci. 127 (2019) 199–207. doi:10.1016/j.ejps.2018.11.003.

[24] S.-J. Kim, H.-K. Lee, Y.-G. Na, K.-H. Bang, H.-J. Lee, M. Wang, H.-W. Huh, C.-W. Cho, A novel composition of ticagrelor by solid dispersion technique for increasing solubility and intestinal permeability, Int. J. Pharm. 555 (2019) 11–18. doi:10.1016/j.ijpharm.2018.11.038.

[25] R. Huang, J. Han, R. Wang, X. Zhao, H. Qiao, L. Chen, W. Li, L. Di, W. Zhang, J. Li, Surfactant-free solid dispersion of BCS class IV drug in an amorphous chitosan oligosaccharide matrix for concomitant dissolution in vitro - permeability increase, Eur. J. Pharm. Sci. 130 (2019) 147–155. doi:10.1016/j.ejps.2019.01.031.

[26] R. Wang, J. Han, A. Jiang, R. Huang, T. Fu, L. Wang, Q. Zheng, W. Li, J. Li, Involvement of metabolism-permeability in enhancing the oral bioavailability of curcumin in excipient-free solid dispersions co-formed with piperine, Int. J. Pharm. 561 (2019) 9–18. doi:10.1016/j.ijpharm.2019.02.027.

[27] L. Miao, Y. Liang, W. Pan, J. Gou, T. Yin, Y. Zhang, H. He, X. Tang, Effect of supersaturation on the oral bioavailability of paclitaxel/polymer amorphous solid dispersion, Drug Deliv. Transl. Res. 9 (2019) 344–356. doi:10.1007/s13346-018-0582-9.

[28] N. Shah, H. Sandhu, D.S. Choi, H. Chokshi, A.W. Malick, eds., Amorphous Solid Dispersions, Springer New York, New York, NY, 2014. http://link.springer.com/10.1007/978-1-4939-1598-9 (accessed March 11, 2016).

[29] Shin-Etsu Chemical Co.,Ltd, USP Hypromellose Phtalate HPMCP, (2002).

[30] Shin-Etsu Chemical Co.,Ltd, Hypromellose Phthalate NF HPMCP, (2015).

[31] Toorisaka E., Hashida M., Kamiya N., Ono H., Kokazu Y., Goto M., An enteric-coated dry emulsion formulation for oral insulin delivery, J. Controlled Release. 107 (2005) 91–96. doi:10.1016/j.jconrel.2005.05.022.

[32] J.P. Lakshman, Y. Cao, J. Kowalski, A.T.M. Serajuddin, Application of Melt Extrusion in the Development of a Physically and Chemically Stable High-Energy Amorphous Solid Dispersion of a Poorly Water-Soluble Drug, Mol. Pharm. 5 (2008) 994–1002. doi:10.1021/mp8001073.

[33] A.N. Ghebremeskel, C. Vemavarapu, M. Lodaya, Use of surfactants as plasticizers in preparing solid dispersions of poorly soluble API: Selection of polymer–surfactant combinations using solubility parameters and testing the processability, Int. J. Pharm. 328 (2007) 119–129. doi:10.1016/j.ijpharm.2006.08.010.

[34] L.I. Mosquera-Giraldo, N.S. Trasi, L.S. Taylor, Impact of surfactants on the crystal growth of amorphous celecoxib, Int. J. Pharm. 461 (2014) 251–257. doi:10.1016/j.ijpharm.2013.11.057.

[35] J. Chen, J.D. Ormes, J.D. Higgins, L.S. Taylor, Impact of Surfactants on the Crystallization of Aqueous Suspensions of Celecoxib Amorphous Solid Dispersion Spray Dried Particles, Mol. Pharm. 12 (2015) 533–541. doi:10.1021/mp5006245.

[36] N.G. Solanki, K. Lam, M. Tahsin, S.G. Gumaste, A.V. Shah, A.T.M. Serajuddin, Effects of Surfactants on Itraconazole-HPMCAS Solid Dispersion Prepared by Hot-Melt Extrusion I: Miscibility and Drug Release, J. Pharm. Sci. 108 (2019) 1453–1465. doi:10.1016/j.xphs.2018.10.058.

[37] J.P. Canselier, C.H. Lin, N. Gabas, J. Tanori, I. Pezron, D. Clausse, Surfactant effects in crystallization: nucleation and crystal habit of γ-aminobutyric acid, in: R.H. Ottewill, A.R. Rennie (Eds.), Trends Colloid Interface Sci. VIII, Steinkopff, 1994: pp. 174–178.

[38] F. Meng, R. Ferreira, F. Zhang, Effect of surfactant level on properties of celecoxib amorphous solid dispersions, J. Drug Deliv. Sci. Technol. 49 (2019) 301–307. doi:10.1016/j.jddst.2018.11.026.

[39] J. Pawar, A. Tayade, A. Gangurde, K. Moravkar, P. Amin, Solubility and dissolution enhancement of efavirenz hot melt extruded amorphous solid dispersions using combination of polymeric blends: A QbD approach, Eur. J. Pharm. Sci. 88 (2016) 37–49. doi:10.1016/j.ejps.2016.04.001.
[40] S. Kolhe, P.D. Chaudhari, D. More, Dissolution and bioavailability enhancement of efavirenz by hot melt extrusion technique, J. Pharm. 4 (2014) 47–53.
[41] R.N. Kamble, P.P. Mehta, A. Kumar, Efavirenz Self-Nano-Emulsifying Drug Delivery System: In Vitro and In Vivo Evaluation, AAPS PharmSciTech. 17 (2016) 1240–1247. doi:10.1208/s12249-015-0446-2.
[42] R.B. Nawale, U.A. Deokate, S.R. Shahi, P.M. Lokhande, Formulation and characterization of efavirenz nanosuspension by QbD approach, Res. J. Pharm. Technol. 10 (2017) 2960–2972. doi:10.5958/0974-360X.2017.00525.X.
[43] Z.M.M. Lavra, D.P. de Santana, M.I. Ré, Solubility and dissolution performances of spray-dried solid dispersion of Efavirenz in Soluplus, Drug Dev. Ind. Pharm. 43 (2017) 42–54. doi:10.1080/03639045.2016.1205598.
[44] B.N.V. Hari, N. Narayanan, K. Dhevendaran, D. Ramyadevi, Engineered nanoparticles of Efavirenz using methacrylate co-polymer (Eudragit-E100) and its biological effects in-vivo, Mater. Sci. Eng. C. 67 (2016) 522–532. doi:10.1016/j.msec.2016.05.064.
[45] Z.M.M. Lavra, D.P. de Santana, M.I. Ré, Solubility and dissolution performances of spray-dried solid dispersion of Efavirenz in Soluplus, Drug Dev. Ind. Pharm. 43 (2017) 42–54. doi:10.1080/03639045.2016.1205598.
[46] † Nehal A. Kasim, † Marc Whitehouse, † Chandrasekharan Ramachandran, § Marival Bermejo, Hans Lennernäs, ⊥ Ajaz S. Hussain, # Hans E. Junginger, ∇ Salomon A. Stavchansky, + Kamal K. Midha, ⊥ Vinod P. Shah, † Gordon L. Amidon *, Molecular Properties of WHO Essential Drugs and Provisional Biopharmaceutical Classification, (2003). doi:10.1021/mp034006h.
[47] R. Cristofoletti, A. Nair, B. Abrahamsson, D. W. Groot, S. Kopp, P. Langguth, J.E. Polli, V.P. Shah, J.B. Dressman, Biowaiver Monographs for Immediate Release Solid Oral Dosage Forms: Efavirenz, J. Pharm. Sci. 102 (2013) 318–328. doi:10.1002/jps.23380.
[48]European Directorate for the Quality of Medicines & HealthCare (EDQM) , European Pharmacopoeia, 7th Ed., 2012.
[49] M. Donzelli, A. Derungs, M.-G. Serratore, C. Noppen, L. Nezic, S. Krähenbühl, M. Haschke, The Basel Cocktail for Simultaneous Phenotyping of Human Cytochrome P450 Isoforms in Plasma, Saliva and Dried Blood Spots. Clin. Pharmacokinet. 53 (2014) 271–282. doi:10.1007/s40262-013-0115-0.
[50] Y. Zhang, M. Huo, J. Zhou, S. Xie, PKSolver: An add-in program for pharmacokinetic and pharmacodynamic data analysis in Microsoft Excel, Comput. Methods Programs Biomed. 99 (2010) 306–314. doi:10.1016/j.cmpb.2010.01.007.
[51] F.E. Grubbs, Procedures for Detecting Outlying Observations in Samples, Technometrics. 11 (1969) 1–21. doi:10.1080/00401706.1969.10490657.
[52] J.W. Tukey, Comparing Individual Means in the Analysis of Variance, Biometrics. 5 (1949) 99–114. doi:10.2307/3001913.
[53] H. Levene, Robust tests for equality of variances, in: Contrib. Probab. Stat. Essays Honor Harold Hotell., Stanford University Test, 1960: pp. 278–292.
[54] F. Langenbucher, Letters to the Editor: Linearization of dissolution rate curves by the Weibull distribution, J. Pharm. Pharmacol. 24 (1972) 979–981. doi:10.1111/j.2042-7158.1972.tb08930.x.
[55] K.J. Bowers, E. Chow, H. Xu, R.O. Dror, M.P. Eastwood, B.A. Gregersen, J.L. Klepeis, I. Kolossvary, M.A. Moraes, F.D. Sacerdoti, J.K. Salmon, Y. Shan, D.E. Shaw, Scalable Algorithms for Molecular Dynamics Simulations on Commodity Clusters, in: Proc. 2006 ACMIEEE Conf. Supercomput., ACM, New York, NY, USA, 2006. doi:10.1145/1188455.1188544.
[56] L. Martínez, R. Andrade, E.G. Birgin, J.M. Martínez, PACKMOL: A package for building initial configurations for molecular dynamics simulations, J. Comput. Chem. 30 (2009) 2157–2164. doi:10.1002/jcc.21224.

[57] Punčochová K., Ewing A.V., Gajdošová M., Pekárek T., Beránek J., Kazarian S.G., Štěpánek F., The Combined Use of Imaging Approaches to Assess Drug Release from Multicomponent Solid Dispersions, Pharm. Res. 34 (2017) 990–1001. doi:10.1007/s11095-016-2018-x.

[58] F. Tres, K. Treacher, J. Booth, L.P. Hughes, S.A.C. Wren, J.W. Aylott, J.C. Burley, Real time Raman imaging to understand dissolution performance of amorphous solid dispersions, J. Controlled Release. 188 (2014) 53–60. doi:10.1016/j.jconrel.2014.05.061.

[59] J.M. Miller, A. Beig, B.J. Krieg, R.A. Carr, T.B. Borchardt, G.E. Amidon, G.L. Amidon, A. Dahan, The Solubility–Permeability Interplay: Mechanistic Modeling and Predictive Application of the Impact of Micellar Solubilization on Intestinal Permeation, Mol. Pharm. 8 (2011) 1848–1856. doi:10.1021/mp200181v.

[60] J.M. Miller, A. Beig, R.A. Carr, J.K. Spence, A. Dahan, A Win–Win Solution in Oral Delivery of Lipophilic Drugs: Supersaturation via Amorphous Solid Dispersions Increases Apparent Solubility without Sacrifice of Intestinal Membrane Permeability, Mol. Pharm. 9 (2012) 2009–2016. doi:10.1021/mp300104s.

[61] A. Beig, N. Fine-Shamir, D. Lindley, J.M. Miller, A. Dahan, Advantageous Solubility-Permeability Interplay When Using Amorphous Solid Dispersion (ASD) Formulation for the BCS Class IV P-gp Substrate Rifaximin: Simultaneous Increase of Both the Solubility and the Permeability, AAPS J. 19 (2017) 806–813. doi:10.1208/s12248-017-0052-1.

[62] K.J. Frank, U. Westedt, K.M. Rosenblatt, P. Hölig, J. Rosenberg, M. Mägerlein, G. Fricker, M. Brandl, The amorphous solid dispersion of the poorly soluble ABT-102 forms nano/microparticulate structures in aqueous medium: impact on solubility, Int. J. Nanomedicine. 7 (2012) 5757–5768. https://doi.org/10.2147/IJN.S36571.

[63] J. Chen, L.I. Mosquera-Giraldo, J.D. Ormes, J.D. Higgins, L.S. Taylor, Bile Salts as Crystallization Inhibitors of Supersaturated Solutions of Poorly Water-Soluble Compounds, Cryst. Growth Des. 15 (2015) 2593–2597. https://doi.org/10.1021/acs.cgd.5b00392.

[64] J. Chen, J.D. Ormes, J.D. Higgins, L.S. Taylor, Impact of Surfactants on the Crystallization of Aqueous Suspensions of Celecoxib Amorphous Solid Dispersion Spray Dried Particles, Mol. Pharm. 12 (2015) 533–541. https://doi.org/10.1021/mp5006245.

[65] Sigma-Aldrich, Polysorbate 80, Product information, (1996).

[66] Physical properties of Sugar Esters, (n.d.). http://www.mfc.co.jp/english/physical.htm (accessed April 5, 2019).

[67] Type of Sugar Esters, http://www.mfc.co.jp/english/ryoto_se/seihin.htm (accessed April 5, 2019).

[68] H. Musther, A. Olivares-Morales, O.J.D. Hatley, B. Liu, A. Rostami Hodjegan, Animal versus human oral drug bioavailability: Do they correlate?, Eur. J. Pharm. Sci. 57 (2014) 280–291. doi:10.1016/j.ejps.2013.08.018.

[69] X. Cao, S.T. Gibbs, L. Fang, H.A. Miller, C.P. Landowski, H.-C. Shin, H. Lennernas, Y. Zhong, G.L. Amidon, L.X. Yu, D. Sun, Why is it Challenging to Predict Intestinal Drug Absorption and Oral Bioavailability in Human Using Rat Model, Pharm. Res. 23 (2006) 1675–1686. doi:10.1007/s11095-006-9041-2.

[70] J.H. Lin, Species similarities and differences in pharmacokinetics, Drug Metab. Dispos. Biol. Fate Chem. 23 (1995) 1008–1021.

[71] J.M. DeSesso, C.F. Jacobson, Anatomical and physiological parameters affecting gastrointestinal absorption in humans and rats, Food Chem. Toxicol. 39 (2001) 209–228.

[72] T.T. Kararli, Comparison of the gastrointestinal anatomy, physiology, and biochemistry of humans and commonly used laboratory animals, Biopharm. Drug Dispos. 16 (1995) 351–380. doi:10.1002/bdd.2510160502.

[73] E.L. McConnell, A.W. Basit, S. Murdan, Measurements of rat and mouse gastrointestinal pH, fluid and lymphoid tissue, and implications for in-vivo experiments, J. Pharm. Pharmacol. 60 (2008) 63–70. doi:10.1211/jpp.60.1.0008.

[74] S. Saphier, A. Rosner, R. Brandeis, Y. Karton, Gastro intestinal tracking and gastric emptying of solid dosage forms in rats using X-ray imagining, Int. J. Pharm. 388 (2010) 190–195. doi:10.1016/j.ijpharm.2010.01.001.

[75] R. Takano, K. Sugano, A. Higashida, Y. Hayashi, M. Machida, Y. Aso, S. Yamashita, Oral Absorption of Poorly Water-Soluble Drugs: Computer Simulation of Fraction Absorbed in Humans from a Miniscale Dissolution Test, Pharm. Res. 23 (2006) 1144–1156. doi:10.1007/s11095-006-0162-4.
[76] S.K. Balani, L.R. Kauffman, F.A. deLuna, J.H. Lin, Nonlinear Pharmacokinetics of Efavirenz (DMP-266), a Potent HIV-1 Reverse Transcriptase Inhibitor, in Rats and Monkeys, Drug Metab. Dispos. 27 (1999) 41–45.
[77] S. Endo, B.I. Escher, K.-U. Goss, Capacities of Membrane Lipids to Accumulate Neutral Organic Chemicals, Environ. Sci. Technol. 45 (2011) 5912–5921. doi:10.1021/es200855w.
[78] N.. E. Ulrich S...Brown, T.N...Watanabe, N...Bronner, G...Abraham, M.H...Goss, K.U., UFZ-LSER database v 3.2 [Internet], (2017). http://www.ufz.de/lserd.

9 Supplement

9.1 Hot-Melt Extrusion Production Settings

Table 3 Extrusion settings *(for formulations F7-41, others with minor deviations).*

Setting	Value
Screw speed	75 rpm
Feed rate (calibrated)	0.5 % corresponding to 0.75 g/min
Temperature Zone 1 (closest to the entry)	Not heated
Temperature Zone 2	140°C
Temperature Zone 3	140°C
Temperature Zone 4	140°C
Temperature Zone 5 (closest to exit)	150°C

9.2 Produced Formulations

Table 4 Produced formulations containing additional polymers*. The nominal drug load of efavirenz was 33.3%.*

Formulation	Additional polymers		
	Weight fraction HPMCP HP 50 [%]	Additional polymer	Weight fraction additional polymer [%]
F1	90	PEG 6000	10
F2	85	PEG 6000	15
F3	80	PEG 6000	20
F4	70	PEG 6000	30
F5	90	Soluplus	10
F6	85	Soluplus	15
F7	90	Kollicoat IR	10

F8	85	Kollicoat IR	15
F9	80	Kollicoat IR	20
F10	90	PEO MW 100.000	10
F11	85	PEO MW 100.000	15

Table 5 Produced formulations containing additional surfactants.

Formulation	Additional surfactant	Additional surfactant [w/w %]	Nominal drug load [w/w %]
F12	Polysorbate 80	-	33.3
F14	Polysorbate 80	10	30.3
F15	Polysorbate 80	5	31.7
F16	Polysorbate 80	2.5	32.5
F17	Polysorbate 80	1.25	32.8
F18	Sucrose Palmitate	10	30.3
F19	Mix 1[a]	2.5	32.5
F20	Mix 1[a]	5	31.7
F21	Mix 1[a]	1.25	32.8
F13	Kolliphor EL		33.3
F22	Kolliphor EL	10	30.3
F23	Kolliphor EL	5	31.7
F24	Kolliphor EL	20	27.8
F25	Kolliphor EL	15	28.9
F26	Kolliphor EL	2.5	32.5
F27	Mix 2[b]	10	30.3
F28	Mix 2[b]	5	31.7
F29	Mix 2[b]	2.5	32.5
F30	Mix 2[b]	1.25	32.8

[a]Mix 1 consisting of polysorbate to Kolliphor EL ratio 1:1.
[b]Mix 2 consisting of Kolliphor EL, polysorbate 80, ethyldiglycol, and Kolliphor TPGS ratio 5:5:5:1.

Table 6 Produced formulations other than in Table 1 during optimization screening. *Formulations contained additional surfactants sucrose palmitate, polysorbate 80 or ethyldiglycol.*

Formulation	Polymer	Added fraction of sucrose palmitate in solid	Added surfactants in liquid	Added fraction of surfactants in liquid feed	Nominal drug load

		feed [w/w%]	feed	[w/w %]	[w/w %]
F32	HPMCP HP55	10	Mix 3[c]	5	28.9
F33	HPMCP HP55	10	Mix 3[c]	2.5	29.3
F35	HPMCP HP55	10	Tween 80	10	27.8
F41	HPMCP HP55	5	Tween 80	10	28.9

[c]Mix 3 consisting of polysorbate 80 and ethyldiglycol ratio 2:1.

9.3 Details on Administered Formulations

Table 7 Formulations used in rat pharmacokinetic experiments.

Formulation	Type	Ingredients	Production Method	Dose [mg/kg]	Carrier Medium	Particle size [µm]	n
F0	Investigational	Efavirenz HPMCP HP55	HME	10	Suspended in water, 1 ml	90	2
F0, dissolved	Investigational	Efavirenz HPMCP HP55	HME	10	Dissolved in buffer at pH 7, 10 ml/kg	-	3
F40	Investigational	Efavirenz HPMCP HP50 Sucrose palmitate Polysorbate 80	HME	10	Suspended in water, 0.1% polysorbate 20, 1 ml	90	4
Stocrin	Marketed formulation	Efavirenz Additives	-	10	Suspended in water, 0.1% polysorbate 20, 1 ml	90	3
i.v. formulation	Investigational Reference	Efavirenz PEG 200 DMSO Saline 0.9%	Liquid, sterile	5	0.9% NaCl, PEG400, DMSO	-	3
F0, physical mixture	Investigational Reference	Efavirenz HPMCP HP55	Blending	10	Suspended in water, 0.1% polysorbate 20, 1 ml	125	3

9.4 Mass Spectrometry Method Details

Table 8 Mass spectrometry method settings.

Setting	Value
Method duration	5.5 min

Transition efavirenz	313.973 → 69.000 Da
Transition efavirenz deuterated	317.951 → 247.900 Da
Ion spray voltage	-4200 V
Source temperature	700°C

9.5 Mechanistic Dissolution Data Fitting Details

A graphical representation of the compartments and rate constants is provided in ***Figure 7***.

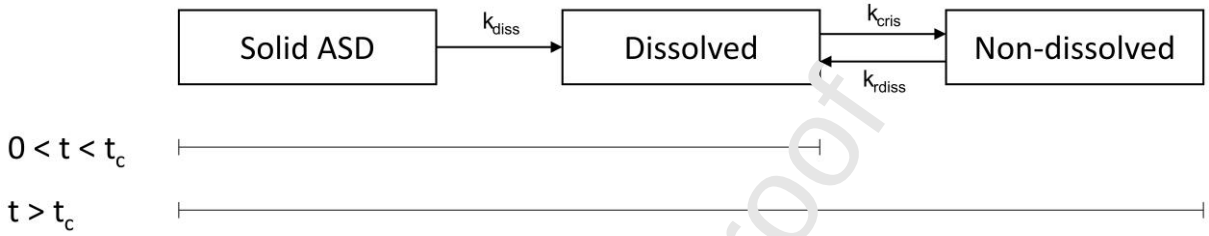

Figure 7: Schematic illustration of the piecewise system of ordinary differential equations (ODE) used for fitting measured dissolution data. *A different system of ODE was used for times t shorter or larger than the time of crystallization t_c.*

The parameters k_{diss}, k_{crys}, k_{rdiss}, *d*, *and* t_c of the solution of the piecewise system of ODE were fitted with the following constraints. In first step, suited starting parameters were found by fitting the dissolution data in additional point resulting from linear interpolation between the measured points (step size 4 min) by the Mathematica function "NonlinearModelFit" using the numerical method "NMinimize". In a second step, original dissolution data were fitted with the method "Automatic" using the same Mathematica function and the starting values from the first fitting. Individual data points were weighted according to their inverse value of the squared standard deviation.

Solving eq. 2 resulted in the following expression for *c(t)*:

$$c(t) = \begin{cases} d\, e^{-k_{diss}\, t}\left(e^{k_{diss}\, t} - 1\right), 0 < t < t_c \\ \dfrac{d\, e^{-k_{diss}\, t - k_{diss}\, t_c - (-k_{crys} - k_{rdiss})\, t_c}\, A}{\left((k_{crys} + k_{rdiss})\,(k_{crys} - k_{diss} + k_{rdiss})\right)}, t > t_c \end{cases} \quad \text{Eq. 5}$$

where *A* is defined as

$$A = -e^{k_{diss}\, t + (-k_{crys} - k_{rdiss})\, t}\, k_{crys}^2 + e^{k_{diss}\, t + (-k_{crys} - k_{rdiss})\, t + k_{diss}\, t_c}\, k_{crys}^2 - e^{k_{diss}\, t + (-k_{crys} - k_{rdiss})\, t + k_{diss}\, t_c}\, k_{crys}\, k_{diss} + e^{k_{diss}\, t_c + (k_{crys} - k_{rdiss})\, t_c}\, k_{crys}\, k_{diss} - e^{k_{diss}\, t + (-k_{crys} - k_{rdiss})\, t}\, k_{crys}\, k_{diss} + e^{k_{diss}\, t + (-k_{crys} - k_{rdiss})\, t + k_{diss}\, t_c}\, k_{crys}\, k_{rdiss} - e^{k_{diss}\, t_c + (-k_{crys} - k_{rdiss})\, t_c}\, k_{crys}\, k_{rdiss} + e^{k_{diss}\, t + k_{diss}\, t_c + (-k_{crys} - k_{rdiss})\, t_c}\, k_{crys}\, k_{rdiss} +$$

$$e^{k_{diss}\,t_c\,+\left(-\,k_{crys}\,-k_{rdiss}\right)\,t_c}\,k_{diss}\,k_{rdiss}-\;e^{k_{diss}\,t\,+\,k_{diss}\,t_c\,+\left(-\,k_{cris}\,-k_{rdiss}\right)\,t_c}\,k_{diss}\,k_{rdiss}\,-$$
$$e^{k_{diss}\,t_c\,+\left(-\,k_{crys}\,-k_{rdiss}\right)\,t_c}\,k_{rdiss}^2+\;e^{k_{diss}\,t+\,k_{diss}\,t_c+\left(-\,k_{crys}\,-k_{rdiss}\right)\,t_c}\,k_{rdiss}^2 \qquad \text{Eq. 6}$$

9.6 Physiologically Based Pharmacokinetic Modeling Results

Table 9: PBPK Model parameters.

Parameter	Set value	Fitting result	Fitting start value	Fitting Range	Source
Intestinal Solubility (FaSSIF, human)	0.194 mg/ml				[75]
Fraction unbound (rat)	0.58 %				[76]
Plasma Clearance		10.11 ml/min/kg	10.43 ml/min/kg	0 - 1000 ml/min/kg	[a]
Entero-hepatic plasma clearance		16.81 ml/min/kg	0 ml/min/kg	0 - 1000 ml/min/kg	
Permeability		9.15 E-3cm/min	0.01 cm/min	8 E-3 – 0.012 cm/min	[b]
Lipophilicity		4.45 Log Units	4.54 Log Units	3.63-5.45 Log Units	[c]
Specific intestinal permeability		4.5 cm/s	4.89 cm/s	3.91-5.87 cm/s	[b]
Weibull dissolution shape		[d]	1	1 E-5 - 10	
Weibull dissolution time		[d]	20	1 E-5 - 1440 min	
Dose		[a]	10 mg/kg	0 - 50 mg/kg	

[a] From the non-compartmental analysis of i.v. pharmacokinetic rat data

[b] Calculated from lipophilicity (compare to [c]) within PK-Sim

[c] Membrane partition coefficient calculated from Linear Solvation Energy Relationship (LSER) descriptors [77,78]

[d] Detailed results are listed in ***Table 10***.

Table 10 Fitting results for p.o. PBPK simulated in vivo dissolution Weibull functions.

Formulation	Dissolution Shape [ ]	Dissolution time (50%) Time [min]	Dose [mg/kg]
F0	0.59	1440.00	0.46
F0, predissolved	0.26	1.36	4.53
F0, physical mixture	0.68	110.41	3.45
F40	1.40	281.18	0.59
Marketed	0.43	23.16	3.82

9.7 Molecular Dynamics Results

Table 11: Surfaces of the molecular ensemble (excluding water) in MD simulations. *In scenario I, molecules were arranged randomly, solvated and simulated (dissolved). In scenario II, the randomly molecules were first condensed into particle by a short MD simulation, then solvated and simulated. Both scenarios were carried out with and without surfactants (sucrose palmitate and polylobate 80).*

	Dissolved (scenario I)					Particle (scenario II)			
	w/o surfactants			with surfactants		w/o surfactants		with surfactants	
Time [ns]	0	20	50	0	20	0	20	0	20
Total Area [Å2]	143369	125814	102369	167640	141543	89829	99859	102316	107023
Change 0 → 20 ns [%]	-	-12.2	-	-	-15.6	-	11.2	-	4.6
Change 0 → 50 ns [%]	-		-28.6	-		-	-	-	-

9.8 *In Vivo* Pharmacokinetic Results

Figure 8 shows the times of maximal concentration and maximal concentrations for the different formulations evaluated in rats.

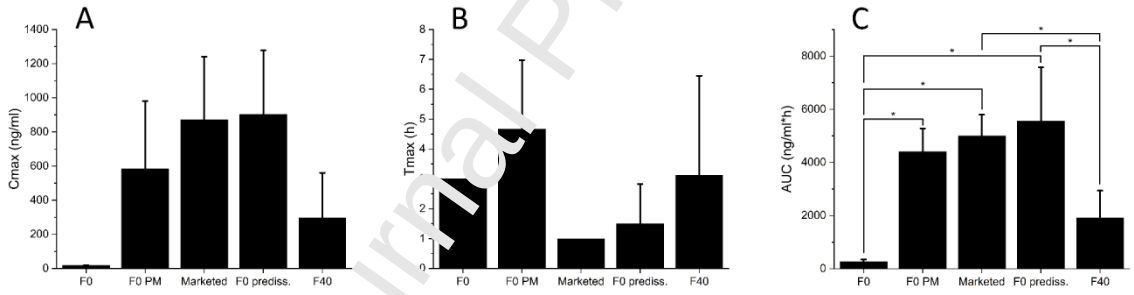

Figure 8: Time of maximal concentration t_{max} (A), maximal concentration (B), and AUC (C) of pharmacokinetic experiments: *Formulation F0 (n=2), predissolved formulation F0 (n=3), formulation F40 (n=4), physical mixture (n=3), and the marketed formulation (n=3) obtained from non-compartmental pharmacokinetic analysis.*

9.9 Solid state characterization

XRPD analysis of Formulation F0 and F40 showed that both formulations were in an amorphous state, as only the halo of amorphous material was detected. Results are shown in Figure 9.

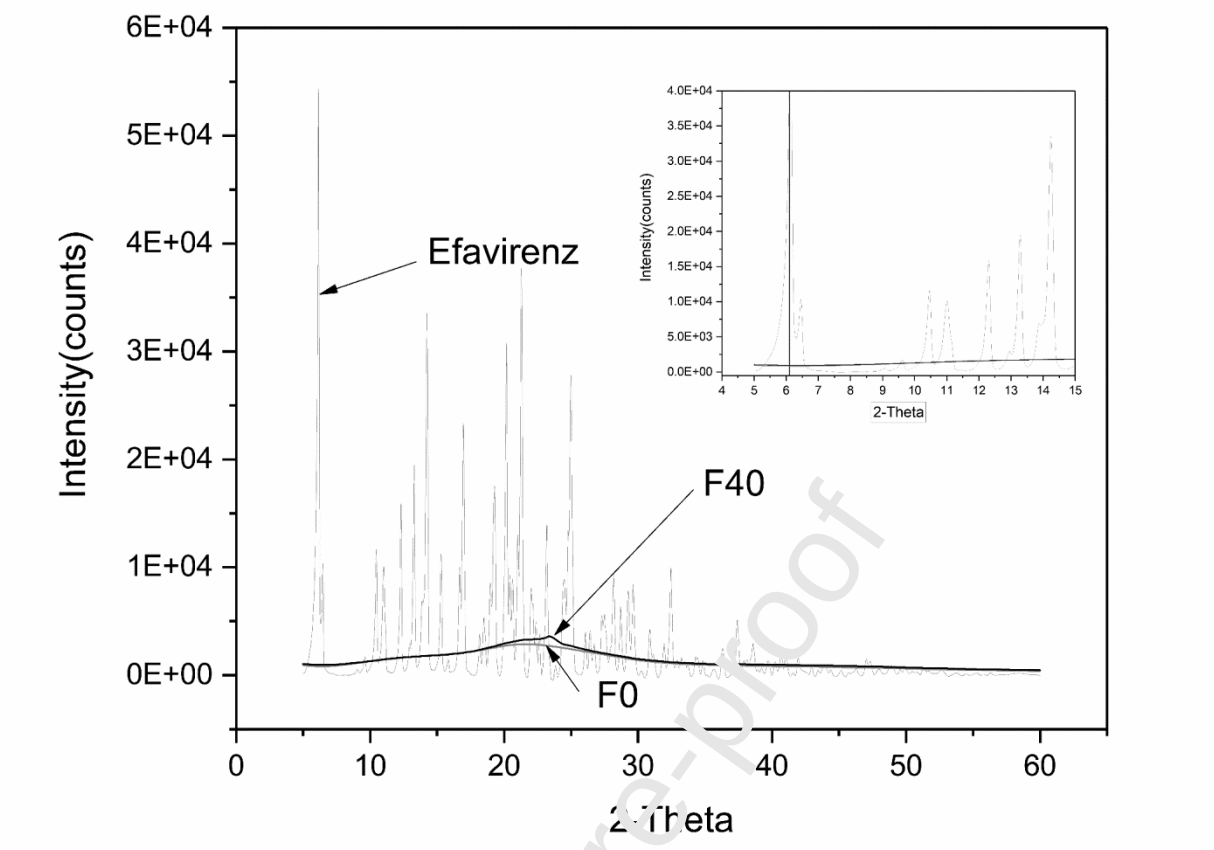

Figure 9: X-ray powder diffractograms of formulation F0 and F40. In addition, the reference of pure efavirenz is shown.

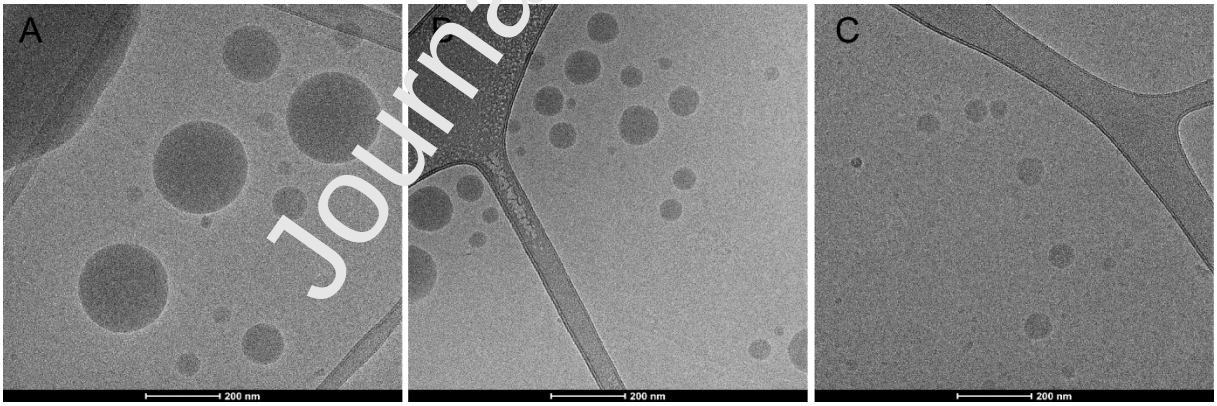

Figure 10: Cryo-TEM images of formuations F37 (A), F31 (B) and F39 (C) by cryogenic electron microscopy. The particle morphology is similar to those seen for formulations F0 and F40.

Graphical abstract